Supplementary Materials for

Accelerated enzyme engineering by machine-learning guided cell-free expression

Grant M. Landwehr, Jonathan W. Bogart, Carol Magalhaes, Eric G. Hammarlund, Ashty S. Karim, and Michael C. Jewett

The PDF file includes:

Table of Contents

Supplementary Figures

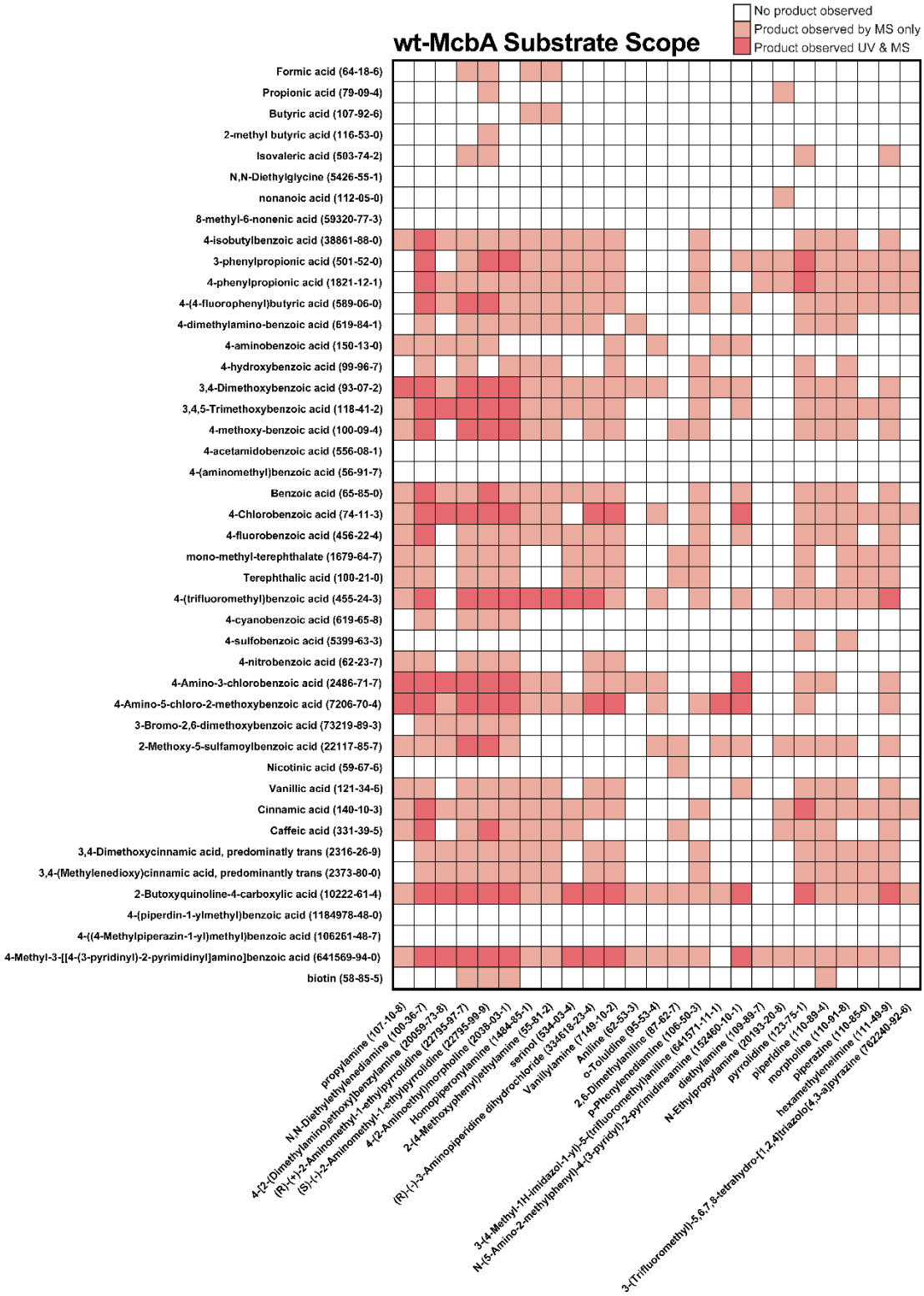

Figure S1. Substrate scope of wt-McbA. This figure key corresponds to the substrate scope presented in **Fig. 2**. All acids (y-axis) and amines (x-axis) tested and their CAS numbers are included. Data shown are from one experiment (n = 1).

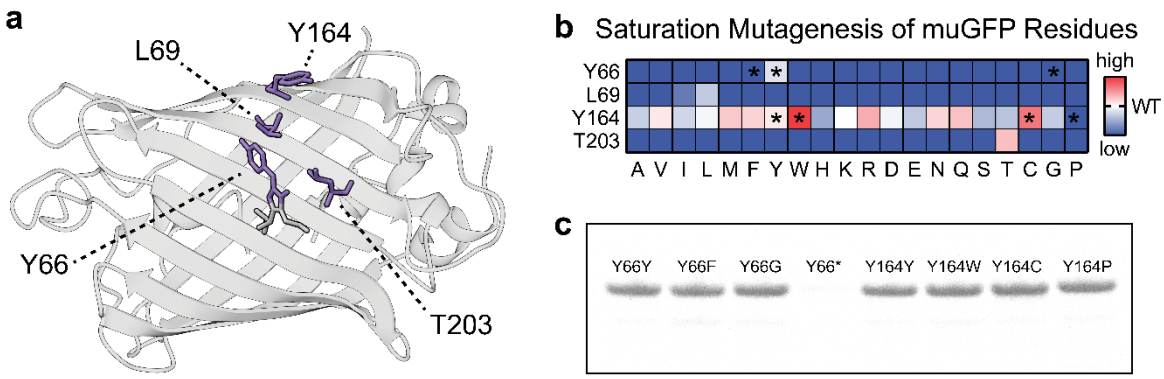

Figure S2. Validation of the cell-free protein expression workflow with muGFP. a, Crystal structure of monomeric ultra-stable green fluorescent protein (muGFP) with residues targeted for saturation mutagenesis highlighted (PDB: 5JZL). **b,** Green fluorescence of single mutants of muGFP generated by site saturation mutagenesis. Data are showing mean fluorescence for *n* = 3 replicates normalized to wild type (wt-muGFP). **c,** Autoradiogram of selected mutants (denoted with asterisks in **b**) showing full-length, soluble proteins are expressed, except in the case when the mutation is a premature stop codon (Y66*). Data shown in the gel are representative of three independent experiments. Source data are provided as a Source Data file.

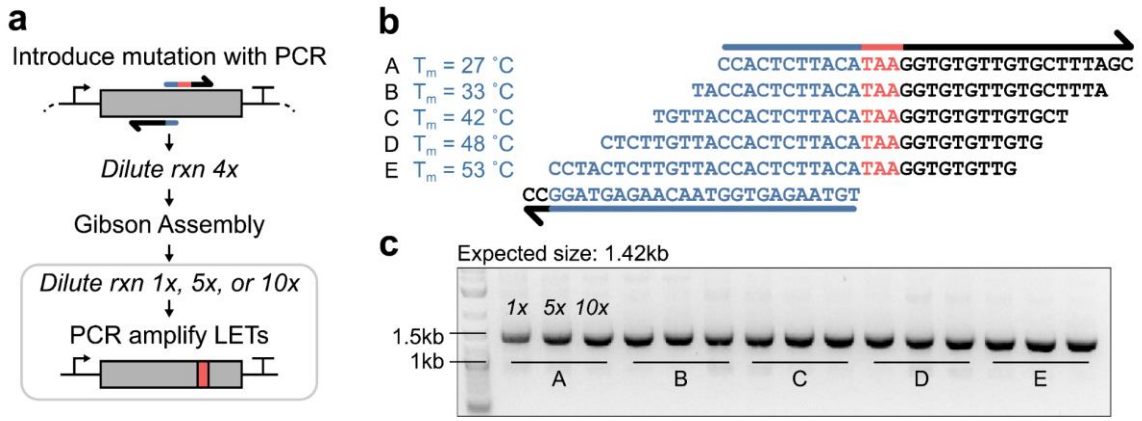

Figure S3. Cell-free DNA assembly efficiency is robust to differences in homologous overlaps of mutagenic primers. a, Schematic of cell-free DNA synthesis and mutation strategy. During protocol development, we considered and made modifications to increase efficiency of the Gibson assembly step: (i) the dilution of the Gibson assembly reaction (serving as the template for the second PCR) and (ii) the amount of homology between the forward and reverse primer in the first PCR. **b,** Five forward primers containing homologous overlaps with a single reverse primer were designed, each overlap differing in T_m by approximately 5 °C. The primers for this experiment were used to introduce a stop codon at Y66 in muGFP. **c,** DNA gel showing the products of the second PCR using primers in **b** and dilutions in **a**. Linear expression templates (LETs) of the expected size are observed. Successful mutagenesis to a stop codon (TAA) was confirmed by Sanger sequencing of the produced LET. Data shown in the gel are representative of three independent experiments.

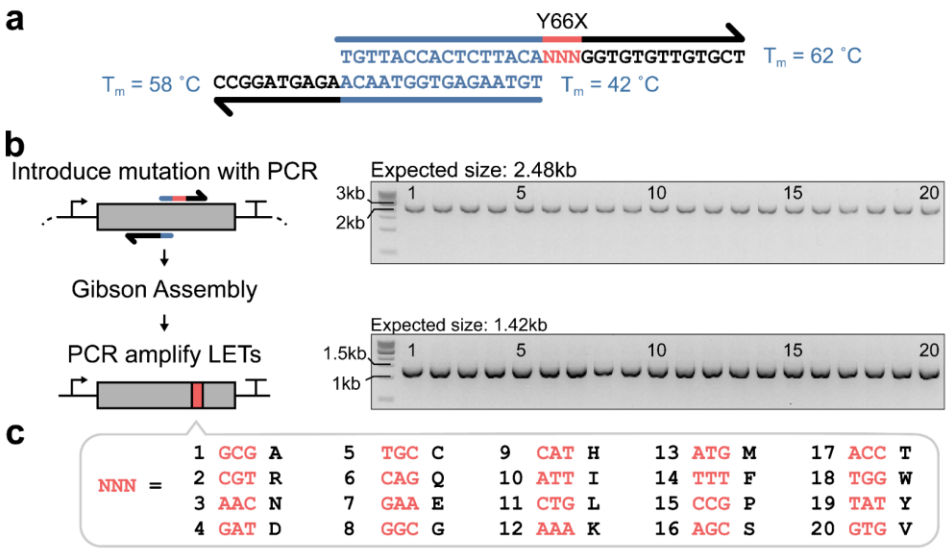

Figure S4. Optimized reaction conditions for cell-free DNA assembly enable site-saturation mutagenesis. a, Primer design schematic. Heuristics are based on primer melting temperatures and were guided by the optimization performed in **Fig. S3.** Shown here are the designed primers for the site saturation of muGFP Y66 with NNN indicating the targeted codon. Briefly, the forward primer containing the desired mutation has a Tm of ~62 °C, the reverse primer has a Tm of ~58 °C, and the homologous overlap between the forward and reverse has a Tm of ~42 °C. **b,** DNA gels demonstrating the expected product size for the two PCR steps of the site saturation of muGFP Y66. Top: linearized plasmid with integrated mutation. Bottom: amplified linear expression template (LET) with integrated mutation. Data shown are representative of three independent experiments. **c,** Amino acid table containing all codons used for site saturation mutagenesis in this study, numbered according to the gels in **b**. The codons correspond to the most prevalent codons found in *E. coli* and were held constant. We elected to not perform codon optimization as (i) tRNAs are supplemented in excess in CFPS reactions so we would not expect a single codon to significantly alter translation and (ii) holding codons constant reduces the complexity of primer design when scaling to numerous mutations.

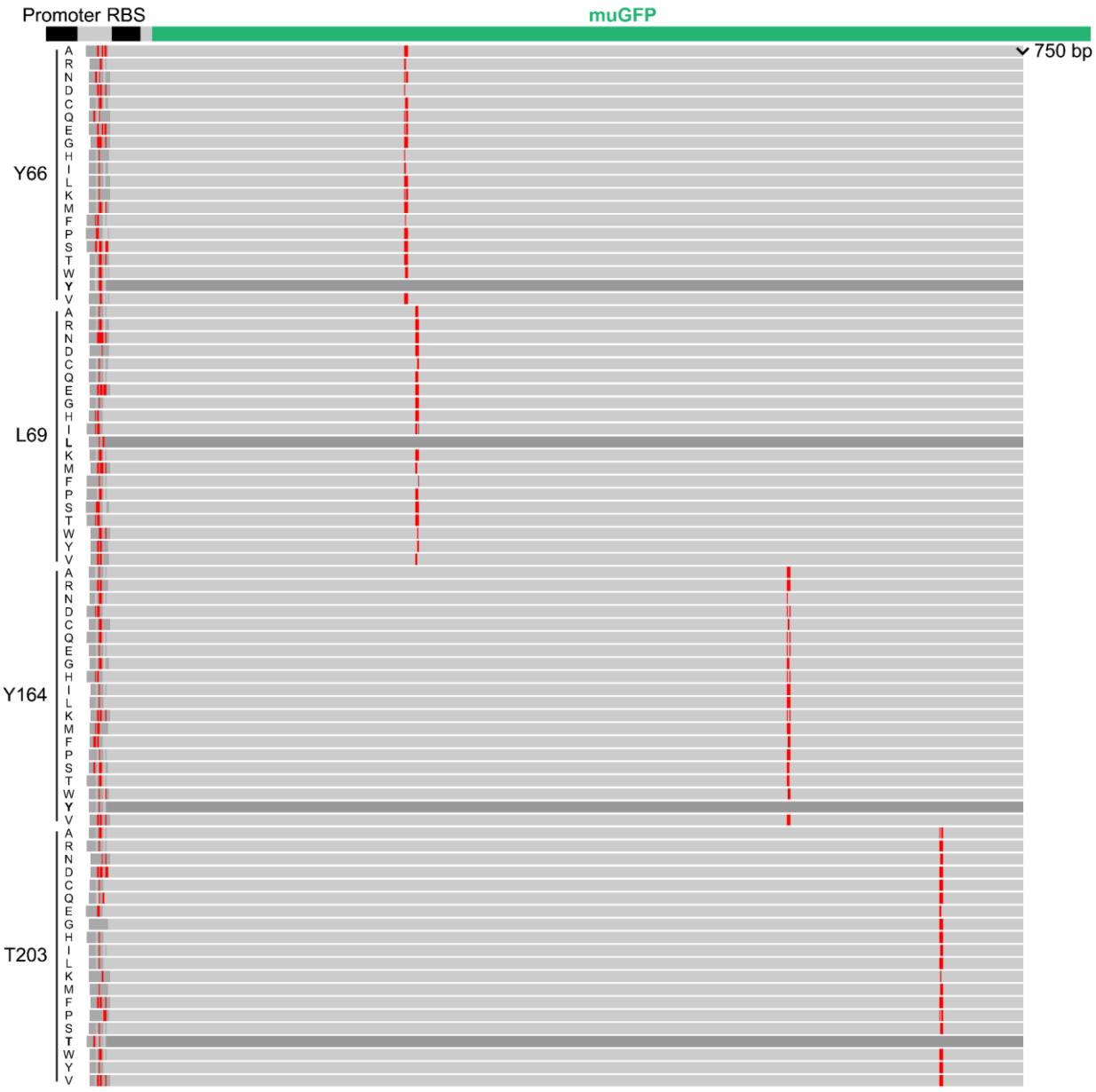

Figure S5. Sequence alignment of muGFP four residue site saturation. The Sanger Sequencing alignment for every muGFP mutant found in **Fig. S2b** generated using our cell-free DNA assembly method aligned to WT muGFP (top; promoter, RBS, and muGFP sequences are highlighted for convenience). Portions of the sequence alignment highlighted in red are mismatches compared to WT muGFP and all correspond to the expected mutation listed on the left-hand side of the alignment.

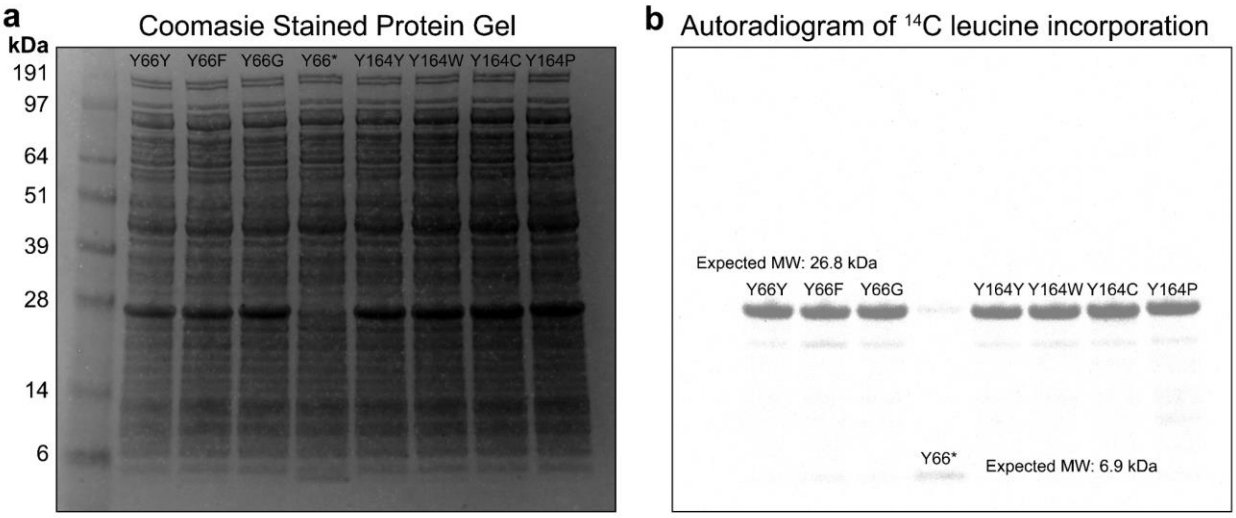

Figure S6. Protein gels of selected muGFP single mutants with variable measured green fluorescence. Complete protein gels of the truncated image shown in **Fig. S2c** depicting selected muGFP mutants from the site saturation mutagenesis screen. Mutants were expressed using CFPS with a radioactive leucine (^{14}C-leucine) to distinguish the expressed protein among the *E. coli* proteome present in CFPS. Two residues were selected (Y66 and Y164) and a stop codon (Y66*) was included as a control to produce a truncated protein. **a**, Coomassie stained protein gel of muGFP expressed in CFPS. **b,** The same gel imaged as an autoradiogram. Data shown are representative of three independent experiments.

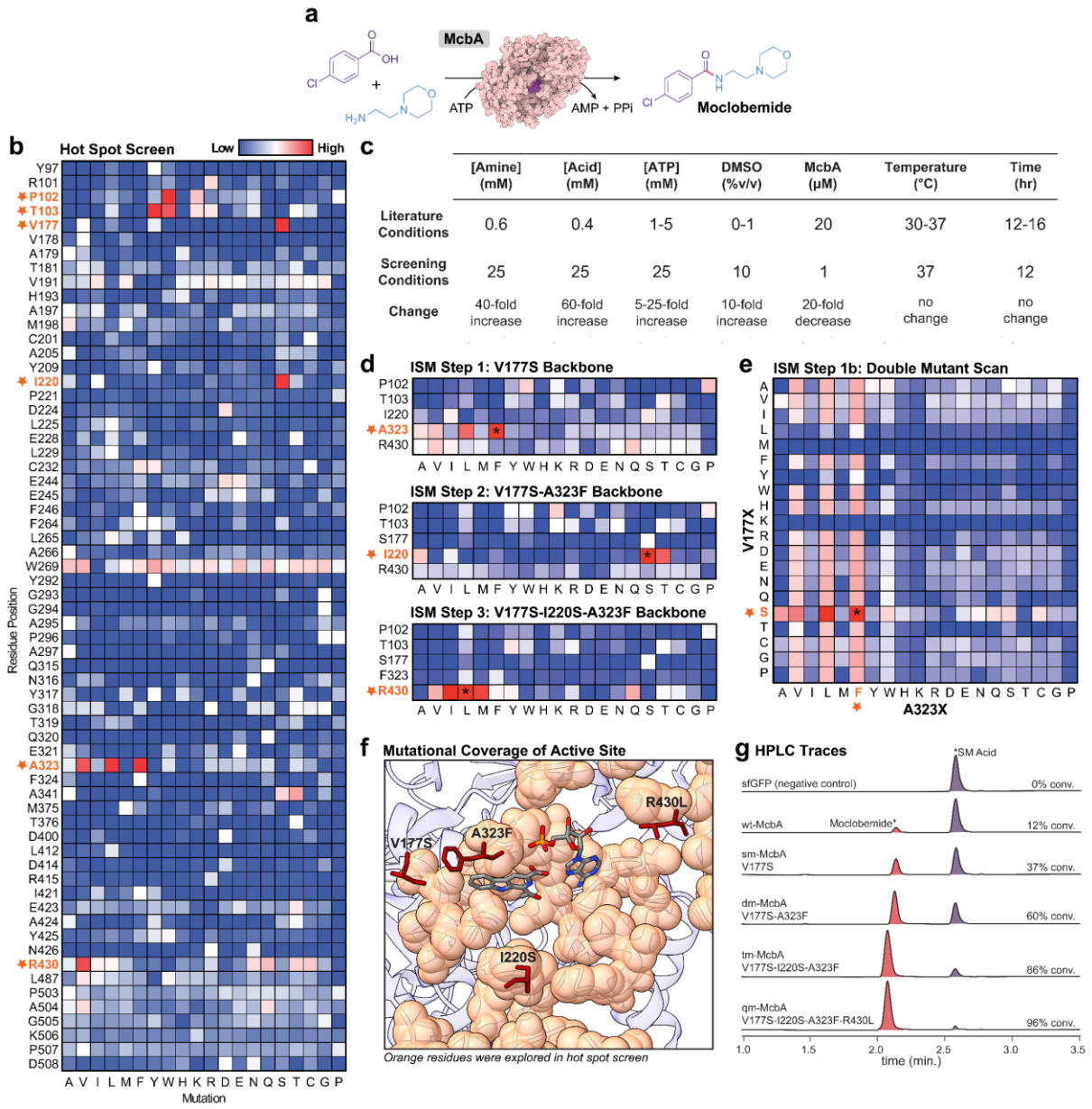

Fig. S7. Engineering campaign for the small-molecule drug moclobemide. a, Reaction scheme for engineering McbA to produce moclobemide. **b,** Hot spot screen of 64 identified residues in McbA showing percent conversion of moclobemide normalized to WT (*n* = 1). Highly mutable sites are starred and included in additional engineering rounds. **c,** Screening conditions for engineering McbA towards more industrially relevant conditions. **d,** Iterative site saturation mutagenesis of residues identified in the HSS, again showing normalized percent conversion of moclobemide (*n* = 1). **e,** Comprehensive double mutant scan of residues identified in the first two rounds of ISM, again showing normalized percent conversion of moclobemide (*n = 1).* **f,** Crystal structure of McbA (PDB: 6SQ8) with bound native substrates. Orange residues highlight the near complete coverage of first shell residues in the active site explored in the HSS. g**,** Reversed-phase (RP)-HPLC traces of moclobemide product (red) and acid substrate (purple) of wt-McbA and engineered mutants. HPLC trace representative of three independent reactions (*n* = 3). Source data are provided as a Source Data file.

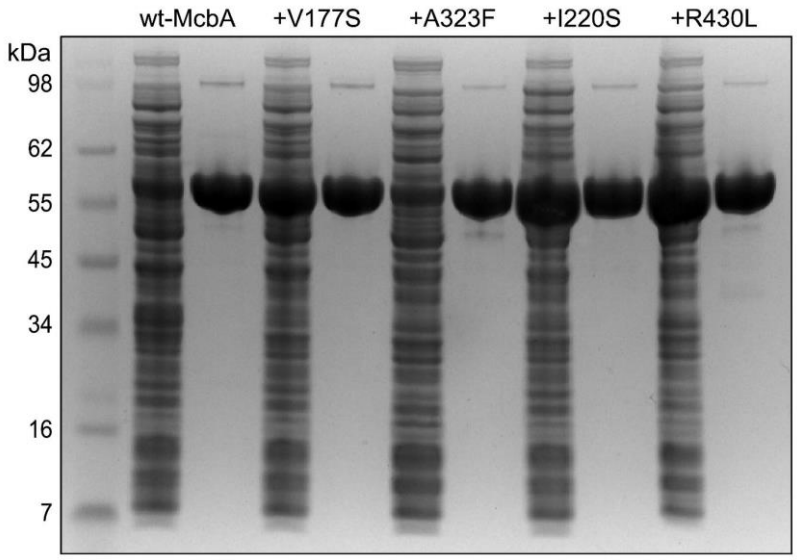

Figure S8. Coomassie stained SDS-PAGE of purified McbA$_{moc}$ variants. McbA variants were expressed in *E. coli* BL21 (DE3) and purified using an N-terminal strep tag. The first lane is the lysate soluble fraction of the overexpressed protein and the second lane is the purified protein. The expected molecular weight was 55.5 kDa, and the purified protein lane was loaded with 10 µg of protein.

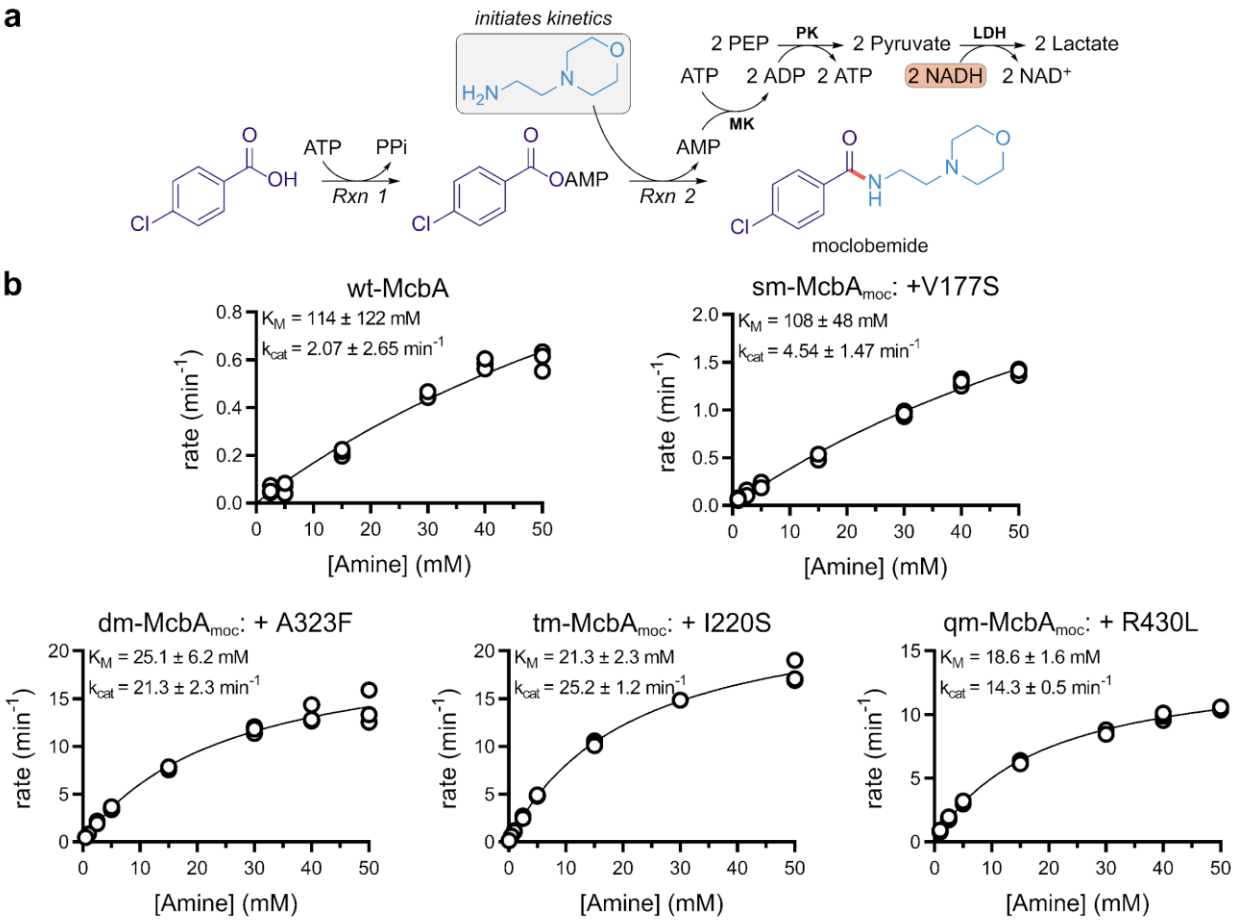

Figure S9. Michaelis-Menten graphs of McbA$_{moc}$ variants. a, The coupled enzymatic reaction scheme we used to measure the Michaelis-Menten kinetics of the amine substrate (4-(2-aminoethyl)morpholine). The reaction was first equilibrated at 30 °C in the presence of the acid (50 mM of 4-chlorobenzoic acid) and ATP (5 mM). The kinetic measurements were initiated by adding varying amounts of amine (0.5 – 50 mM) and the rate was determined by measuring NADH oxidation at 340 nM. **b,** Michaelis-Menten graphs of all McbA$_{moc}$ variants were plotted in GraphPad Prism and fit using the default Michaelis-Menten non-linear regression analysis tool. For both wt-McbA and sm-McbA, we were unable to reach a saturating concentration of amine and therefore have high uncertainty in the estimated kinetic parameters. All data replicates are shown as independent experimental points (n = 3). Source data are provided as a Source Data file.

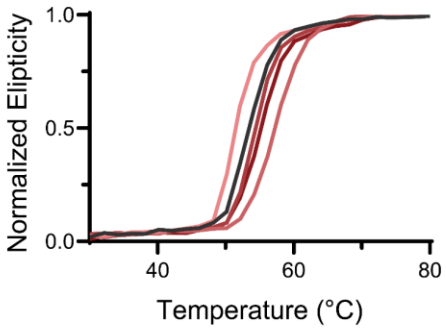

Variant	T_m (°C)
wt-McbA	53.59 ± 0.05
+V177S	51.56 ± 0.08
+A323F	57.46 ± 0.04
+I220S	54.51 ± 0.07
+R430L	55.16 ± 0.05

Figure S10. Melting temperatures of McbA$_{moc}$ variants. Circular dichroism (CD) denaturation curves were min-max normalized for each sample for ease of comparison across mutants. Data traces shown are representative of three independent experiments. Error bars represent standard deviation. Source data are provided as a Source Data file.

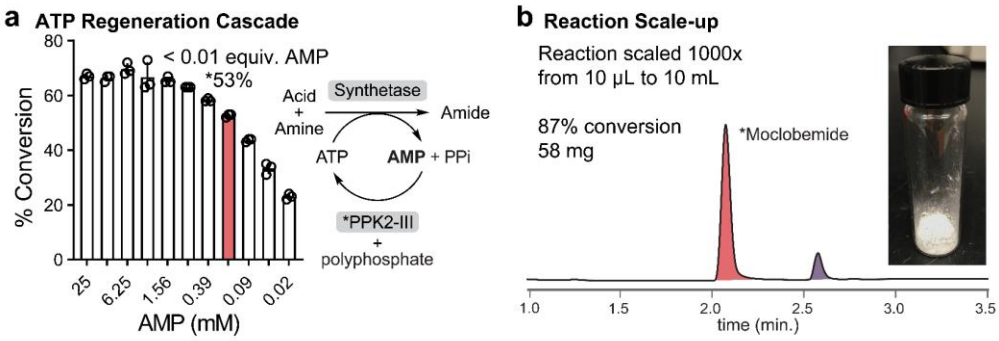

Fig. S11. Preparative-scale synthesis of moclobemide with an engineered McbA. a, An additional ATP regeneration system sustains high percent conversions using low stoichiometric addition of AMP (n = 3)[1,2]. **b,** Preparative scale synthesis of moclobemide with purified product pictured. Source data are provided as a Source Data file.

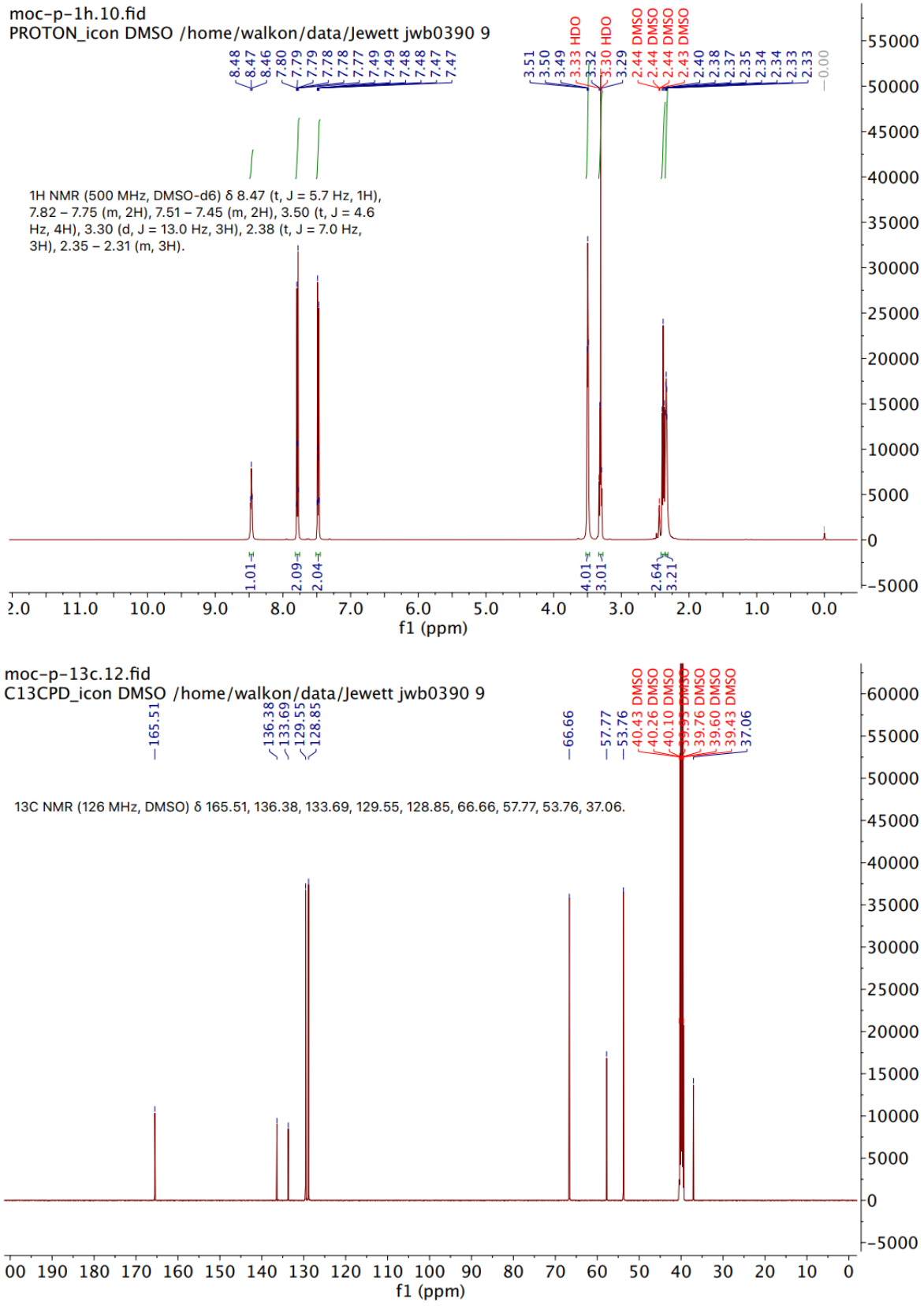

Figure S12. Compound NMR spectra of purified moclobemide synthesized by McbA.

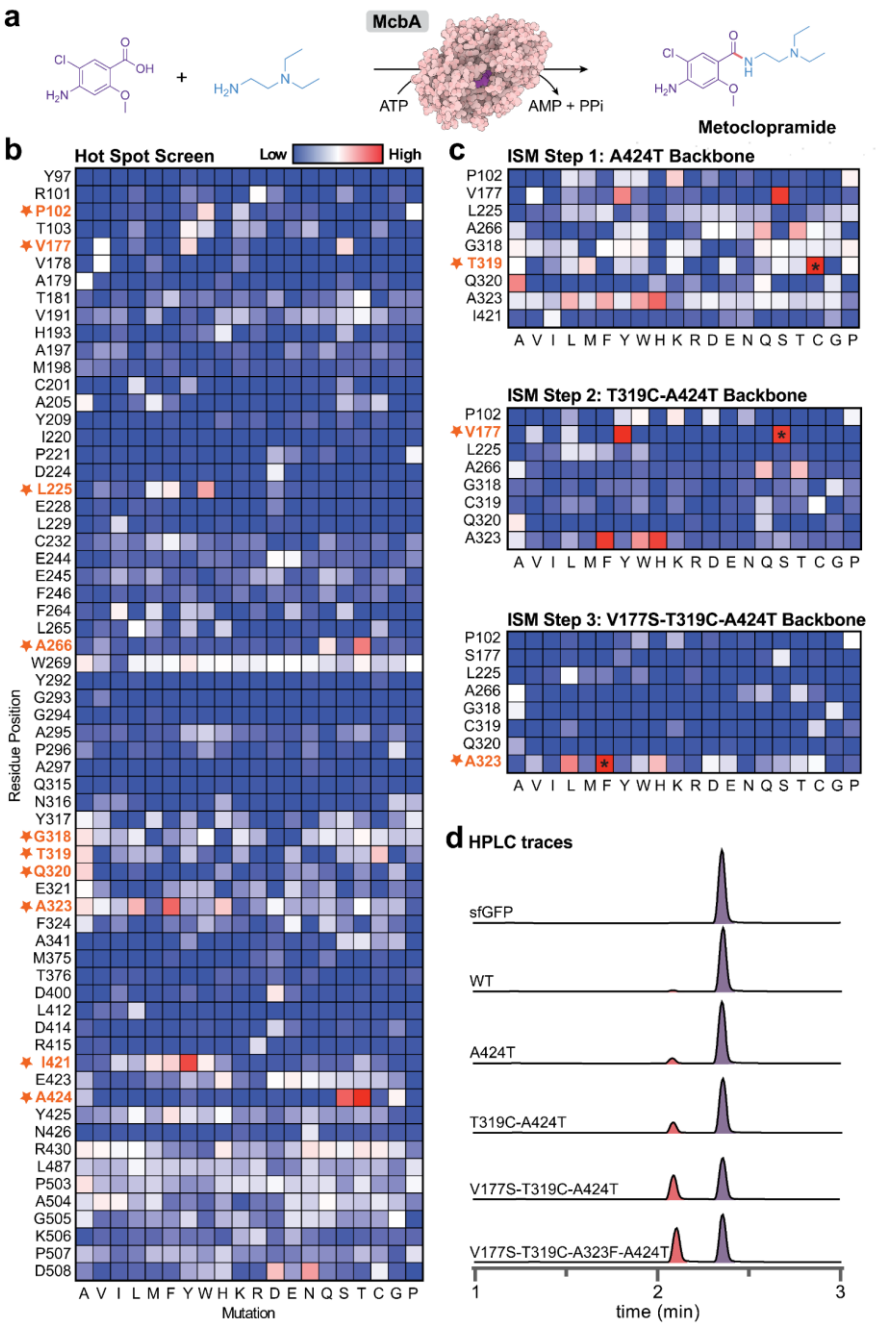

Figure S13. Engineering campaign for the small-molecule drug metoclopramide. a, Reaction scheme for the biosynthesis of metoclopramide using McbA. **b,** HSS of 64 identified residues in McbA showing percent conversion of metoclopramide normalized to WT (n = 1) as determined by absorbance on HPLC. Highly mutable sites are starred and included in additional engineering rounds. **c,** Three additional ISM rounds of residues that were identified in the HSS. The mutation that had the greatest positive impact on activity is starred and was included in the backbone for the next round. **d,** RP-HPLC trace of metoclopramide product (red) and acid substrate (purple) of wt-McbA and engineered mutants. HPLC trace data are representative of three independent experiments. Source data are provided as a Source Data file.

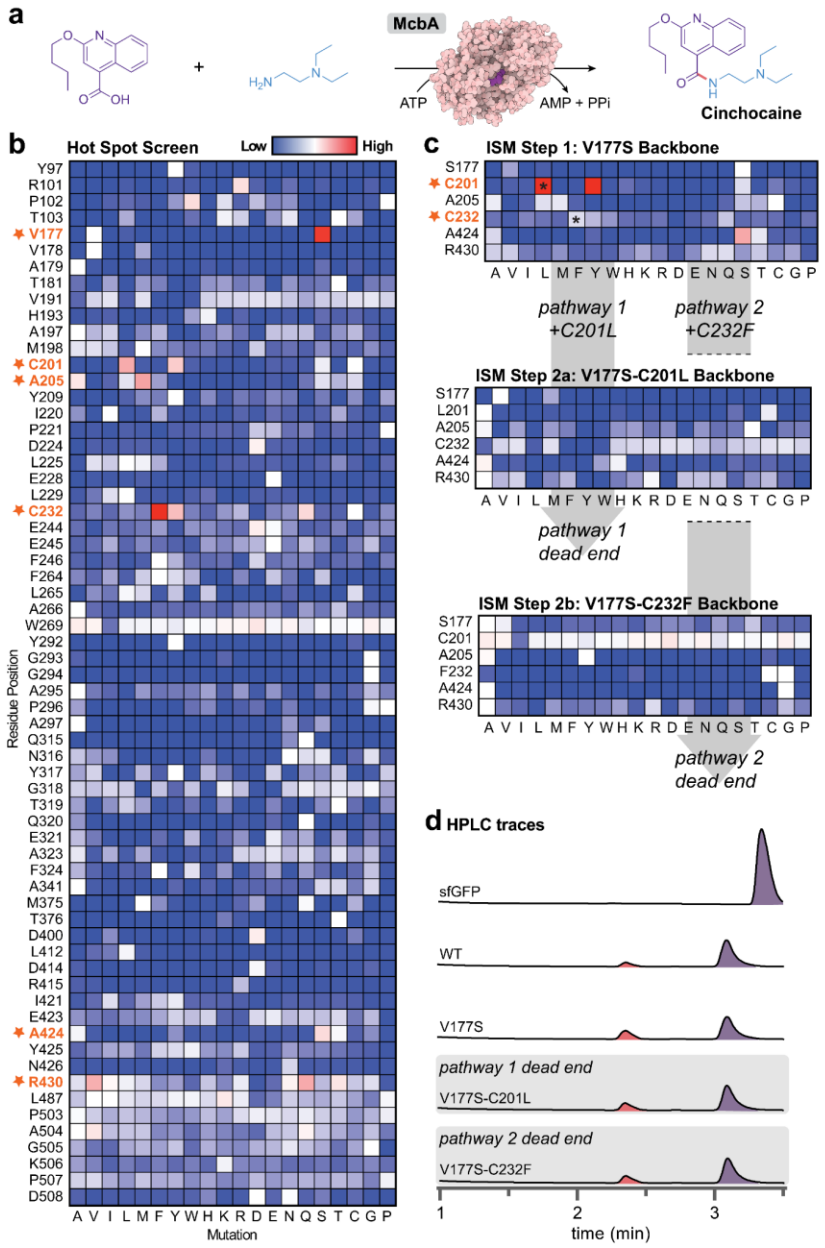

Figure S14. Engineering campaign for the small-molecule drug cinchocaine. a, Reaction scheme for the biosynthesis of cinchocaine using McbA. **b,** HSS of 64 identified residues in McbA showing percent conversion of cinchocaine normalized to WT (*n* = 1) as determined by absorbance on HPLC. Highly mutable sites are starred and included in additional engineering rounds. **c,** After one additional engineering round, we were unable to find an additional beneficial mutation beyond the double mutant (pathway 1). Notably, mutations that were previously observed to be beneficial were no longer in future rounds. To overcome this "dead end", we performed an additional engineering round using a double mutant consisting of the two best mutations found in the HSS (pathway 2). We also could not find additional mutations for this backbone and reached another "dead end". **d,** RP-HPLC trace of cinchocaine product (red) and acid substrate (purple) of wt-McbA and engineered mutants. HPLC trace data are representative of three independent experiments. Source data are provided as a Source Data file.

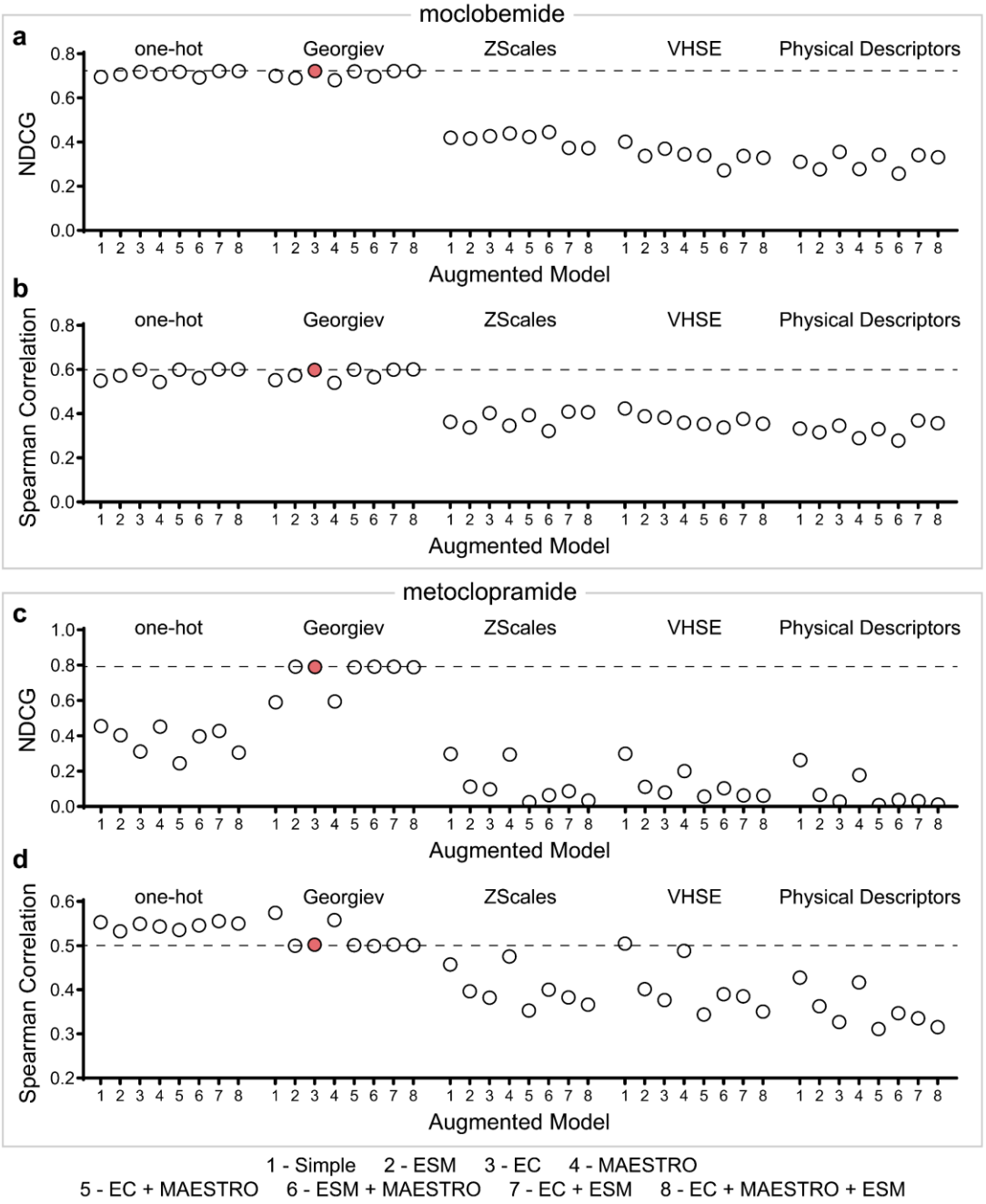

Figure S15. Complete characterization of augmented ridge regression model performance using different combinations of fitness predictors and amino acid encodings. Model performance was evaluated by training a model on single mutant data and testing on the withheld combinatorial data (double, triple, and quadruple mutants) from iterative site saturation mutagenesis. While we explicitly used NDCG as our selection criteria for model performance, we also include the Spearman correlation coefficient to explore the differences in all the models tested. In most instances, these two model performance indicators are closely aligned. The top graphs display NDCG (**a**) and Spearman correlation (**b**) for moclobemide and the bottom graphs display NDCG (**c**) and Spearman correlation (**d**) for metoclopramide. Source data are provided as a Source Data file.

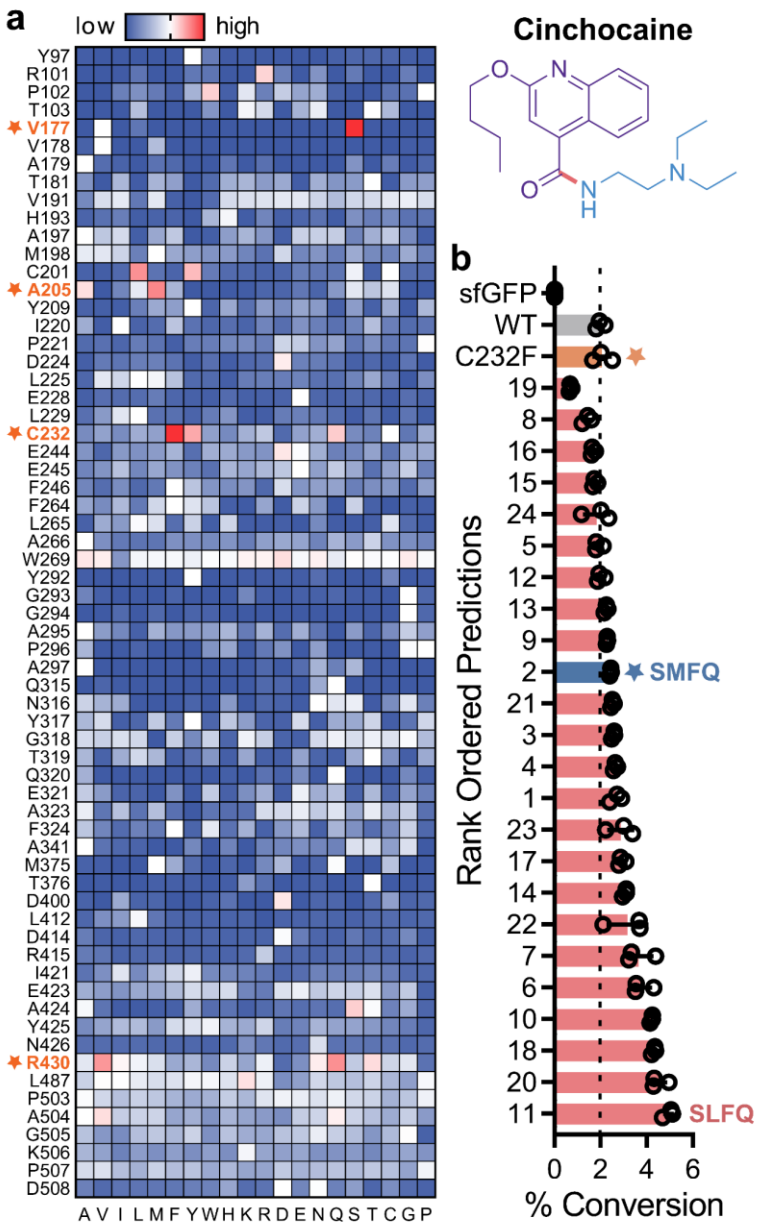

Figure S16. Hot spot screen and machine-learning guided predictions for the biocatalytic synthesis of cinchocaine. a, HSS of 64-site library to identify McbA residues that positively impact cinchocaine synthesis (*n* = 1). Yields are normalized to wt-McbA. **b,** Experimental validation of the top 24 ML-predictions, rank ordered by measured activity (*n* = 3). The variants are labeled by their predicted rank. The most active single mutant from the HSS (orange) and a "rational" design from combining the top four single mutations from the HSS (blue) were also included. The specific mutations corresponding to the ranks in this figure can be found in **Table S2**. Source data are provided as a Source Data file.

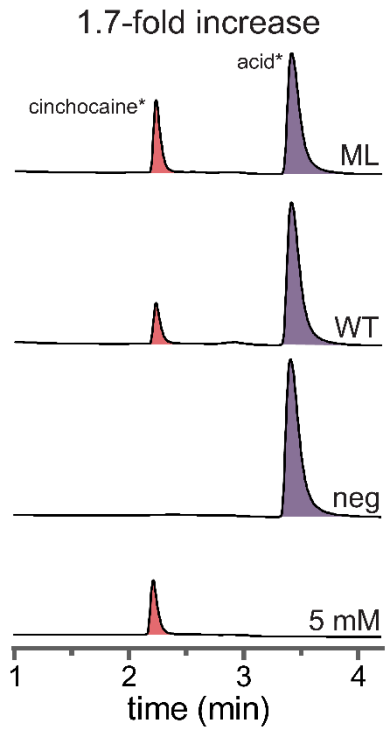

Figure S17. Machine-learning guided predictions have increased activity over wt-McbA for the synthesis of cinchocaine. Reversed-phase (RP)-HPLC traces of cinchocaine product (red) and acid substrate (purple) of wt-McbA ('WT') and the machine learning predicted mutant with the highest activity identified in **Fig. S16** ('ML') compared to an authentic standard. HPLC trace data are representative of three independent experiments.

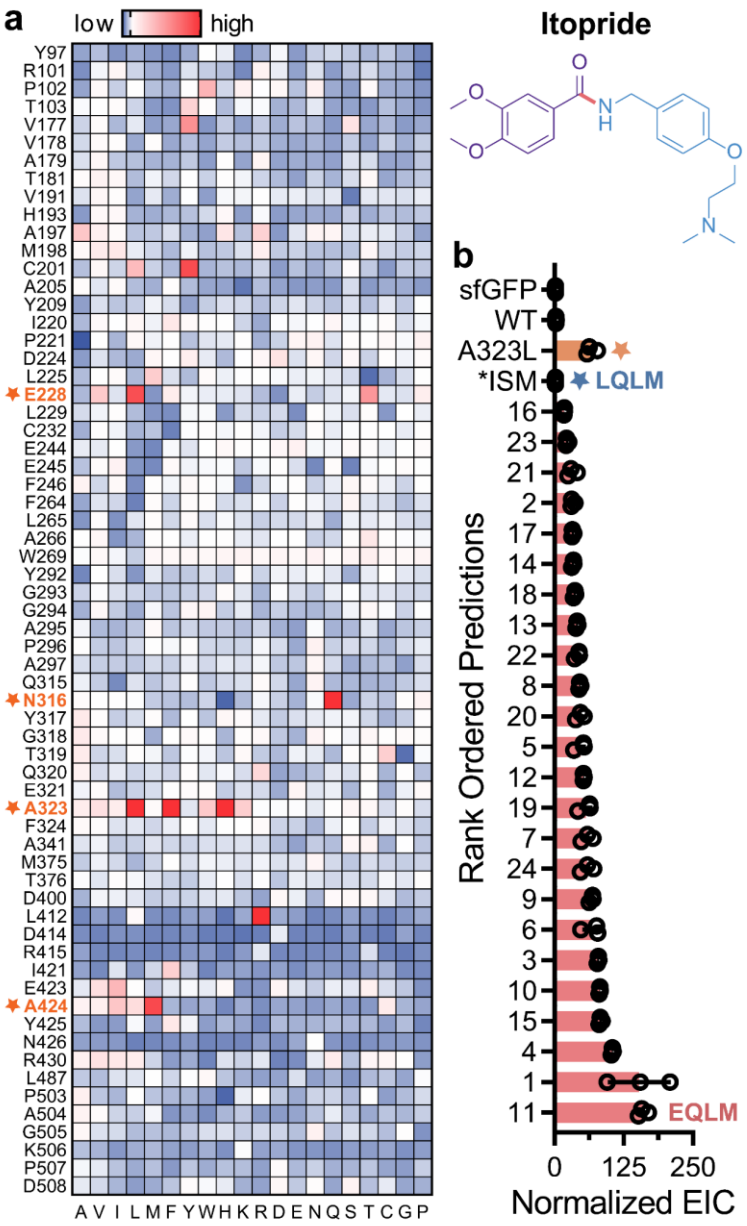

Figure S18. Hot spot screen and machine-learning guided predictions for the biocatalytic synthesis of itopride. a, HSS of 64-site library to identify McbA residues that positively impact itopride synthesis (*n* = 1). Yields are normalized to wt-McbA. **b,** Experimental validation of the top 24 ML-predictions, rank ordered by measured activity (*n* = 3). The variants are labeled by their predicted rank. As wt-McbA and several mutants produce trace amounts only detectable by MSD, we quantified product with EIC (*m*/z of 359.2). The most active single mutant from the HSS (orange) and a "rational" design from combining the top four single mutations from the HSS (blue) were also included. The specific mutations corresponding to the ranks in this figure can be found in **Table S3**. Source data are provided as a Source Data file.

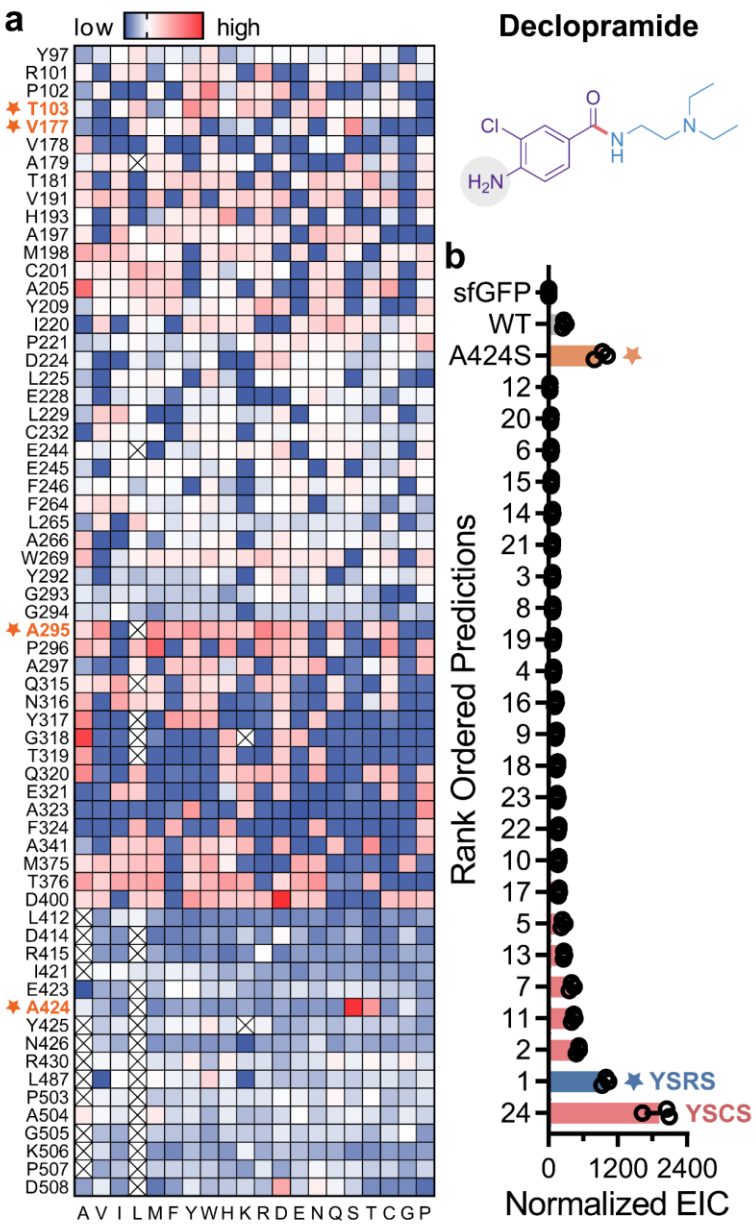

Figure S19. Hot spot screen and machine-learning guided predictions for the biocatalytic synthesis of declopramide. a, HSS of 64-site library to identify McbA residues that positively impact declopramide synthesis (*n* = 1). Yields are normalized to wt-McbA. **b,** Experimental validation of the top 24 ML-predictions, rank ordered by measured activity (*n* = 3). The variants are labeled by their predicted rank. As wt-McbA and several mutants produce trace amounts only detectable by MSD, we quantified product with EIC (*m*/*z* of 270.1). The most active single mutant from the HSS (orange) and a "rational" design from combining the top four single mutations from the HSS (blue) were also included. The specific mutations corresponding to the ranks in this figure can be found in **Table S3.** Source data are provided as a Source Data file.

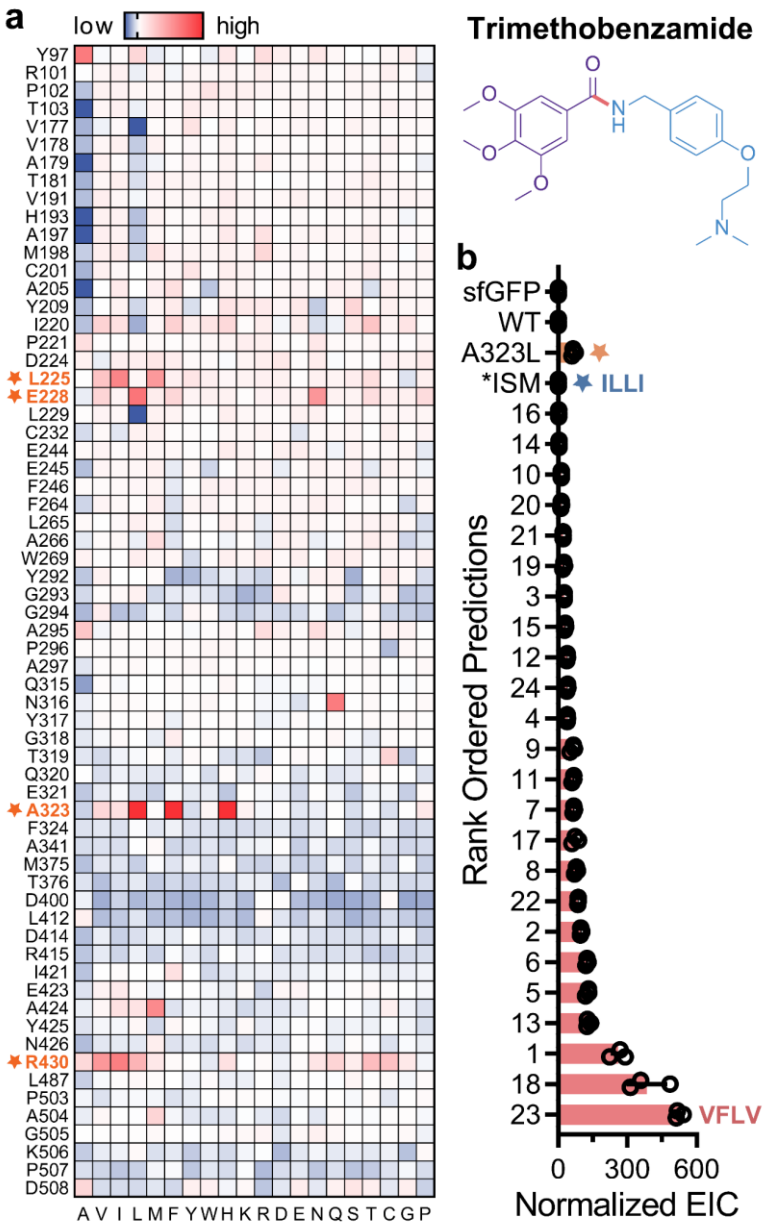

Figure S20. Hot spot screen and machine-learning guided predictions for the biocatalytic synthesis of trimethobenzamide. a, HSS of 64-site library to identify McbA residues that positively impact trimethobenzamide synthesis (*n* = 1). Yields are normalized to wt-McbA. **b,** Experimental validation of the top 24 ML-predictions, rank ordered by measured activity (*n* = 3). The variants are labeled by their predicted rank. As wt-McbA and several mutants produce trace amounts only detectable by MSD, we quantified product with EIC (*m*/z of 389.2). The most active single mutant from the HSS (orange) and a "rational" design from combining the top four single mutations from the HSS (blue) were also included. The specific mutations corresponding to the ranks in this figure can be found in **Table S4.** Source data are provided as a Source Data file.

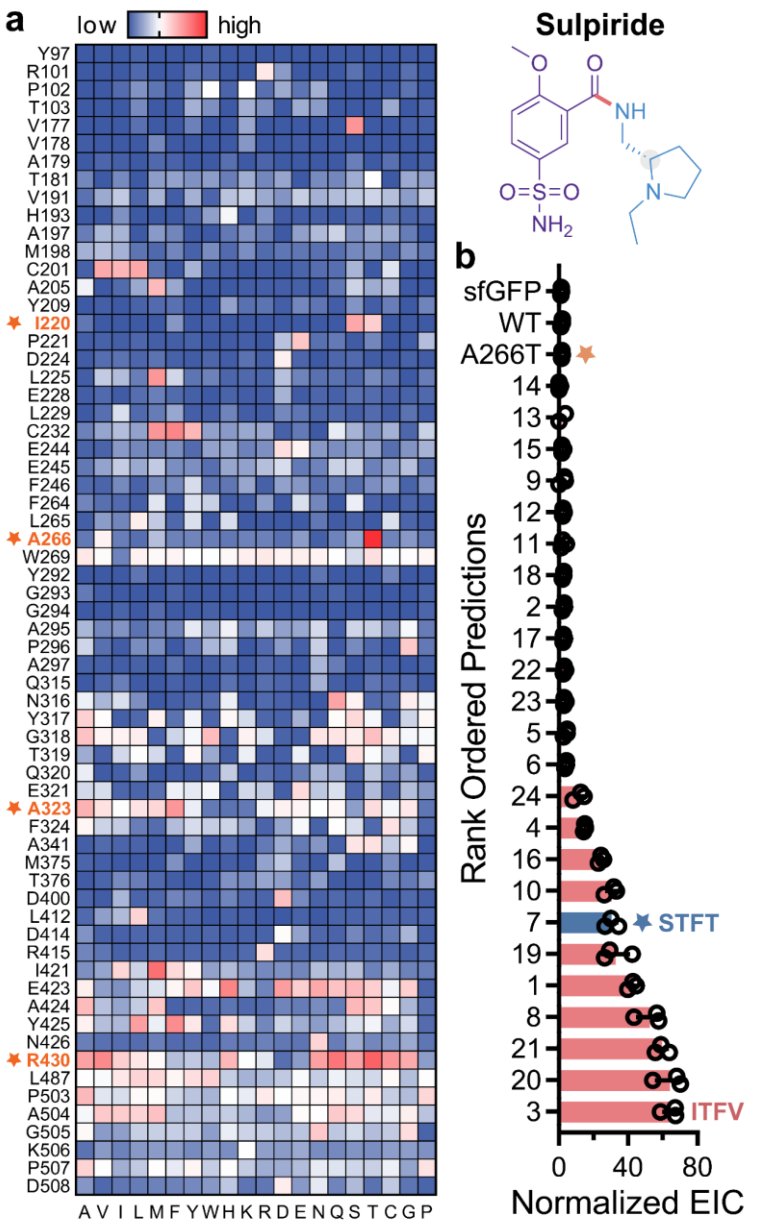

Figure S21. Hot spot screen and machine-learning guided predictions for the biocatalytic synthesis of S-sulpiride. a, HSS of 64-site library to identify McbA residues that positively impact S-sulpiride synthesis (*n* = 1). Yields are normalized to wt-McbA. **b,** Experimental validation of the top 24 ML-predictions, rank ordered by measured activity (*n* = 3). The variants are labeled by their predicted rank. As wt-McbA and several mutants produce trace amounts only detectable by MSD, we quantified product with EIC (*m*/z of 342.1). The most active single mutant from the HSS (orange) and a "rational" design from combining the top four single mutations from the HSS (blue) were also included. The specific mutations corresponding to the ranks in this figure can be found in **Table S4**. Source data are provided as a Source Data file.

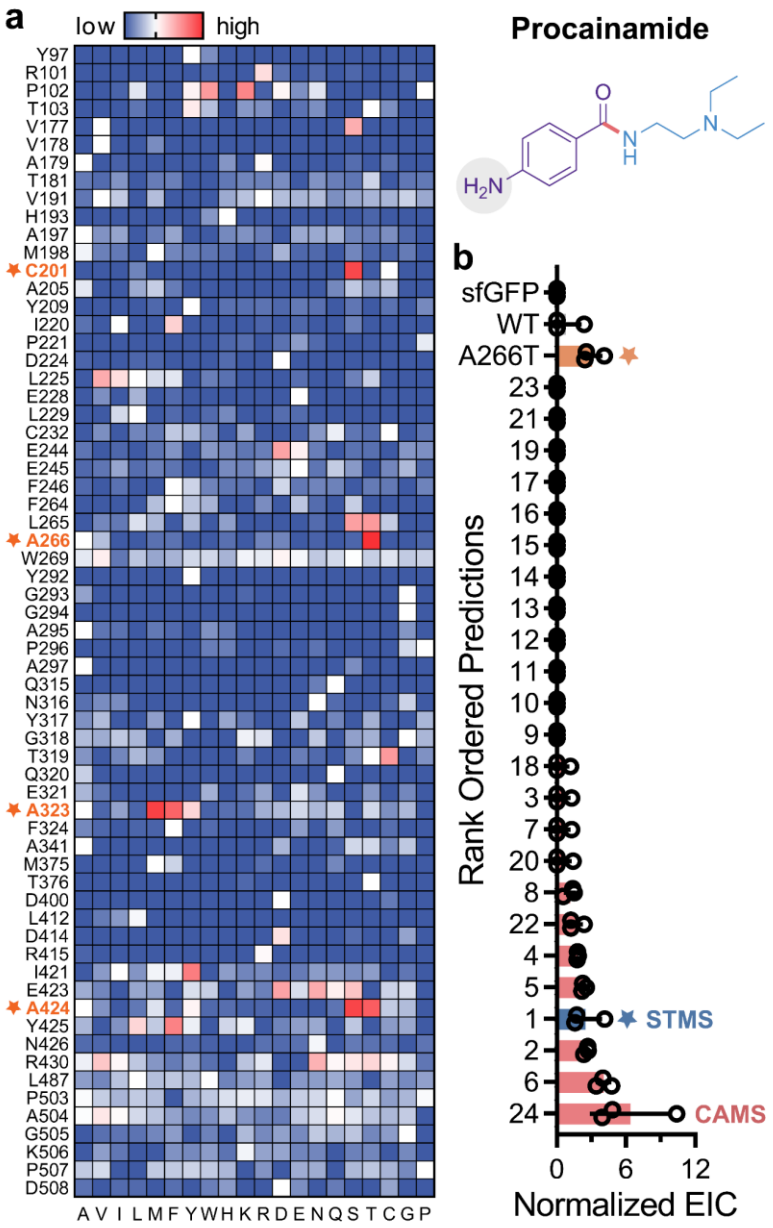

Figure S22. Hot spot screen and machine-learning guided predictions for the biocatalytic synthesis of procainamide. a, HSS of 64-site library to identify McbA residues that positively impact procainamide synthesis (*n* = 1). Yields are normalized to wt-McbA. **b,** Experimental validation of the top 24 ML-predictions, rank ordered by measured activity (*n* = 3). The variants are labeled by their predicted rank. As wt-McbA and several mutants produce trace amounts only detectable by MSD, we quantified product with EIC (*m*/*z* of 236.1). The most active single mutant from the HSS (orange) and a "rational" design from combining the top four single mutations from the HSS (blue) were also included. The specific mutations corresponding to the ranks in this figure can be found in **Table S5.** Source data are provided as a Source Data file.

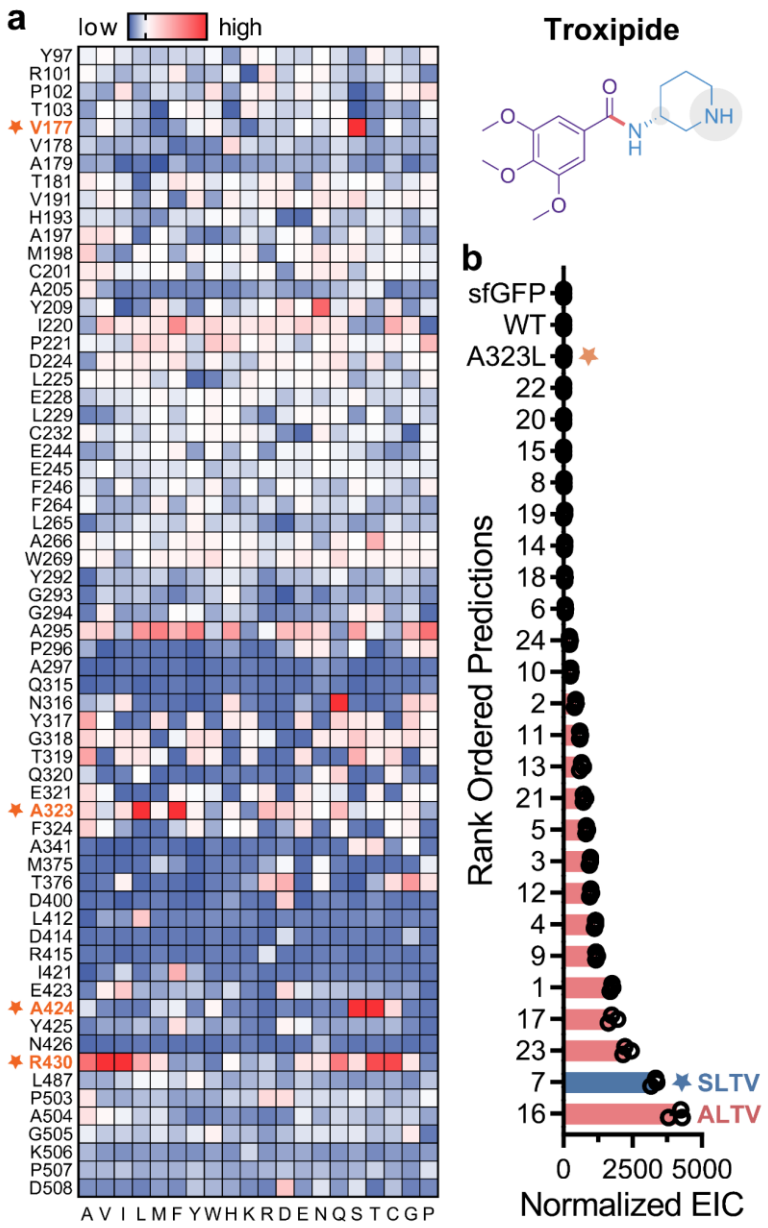

Figure S23. Hot spot screen and machine-learning guided predictions for the biocatalytic synthesis of troxipide. a, HSS of 64-site library to identify McbA residues that positively impact troxipide synthesis (*n* = 1). Yields are normalized to wt-McbA. **b,** Experimental validation of the top 24 ML-predictions, rank ordered by measured activity (*n* = 3). The variants are labeled by their predicted rank. As wt-McbA and several mutants produce trace amounts only detectable by MSD, we quantified product with EIC (*m*/z of 295.1). The most active single mutant from the HSS (orange) and a "rational" design from combining the top four single mutations from the HSS (blue) were also included. The specific mutations corresponding to the ranks in this figure can be found in **Table S5**. Source data are provided as a Source Data file.

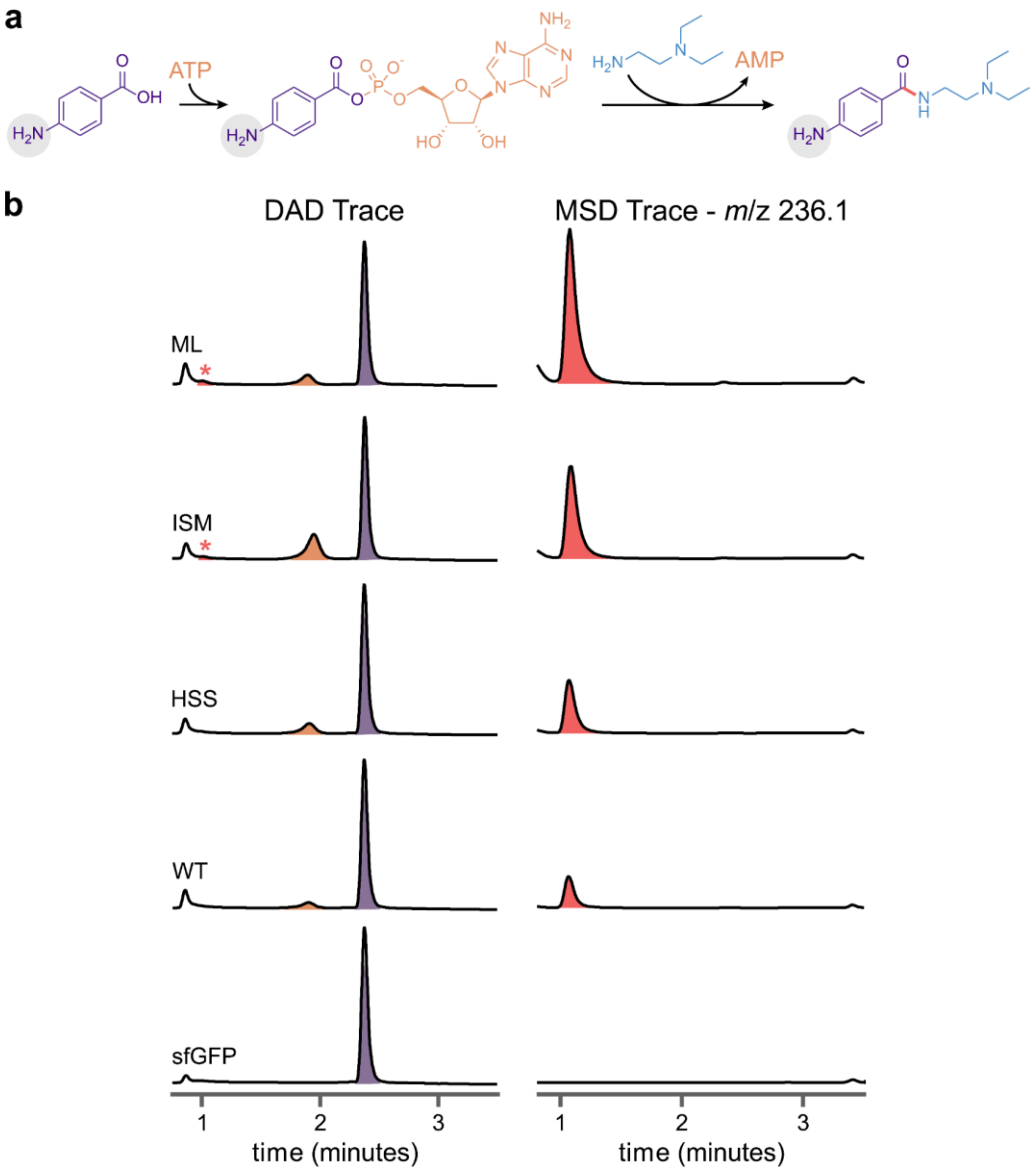

Figure S24. The two-step reaction mechanism of McbA allows us to probe the impact of mutations on the distinct reaction steps. a, The coupled reaction mechanism of ATP-dependent amide bond synthetases, such as McbA, is first the activation of an acid to an acyl-adenylate intermediate followed by substitution with an amine nucleophile. In this example, we focus on the synthesis of procainamide (red) using 4-aminobenzoic acid (purple) and *N,N*-diethylethylenediamine (blue). **b,** Since the acyl-adenylate intermediate (orange) is also measurable by DAD (245nm), we can compare how different mutations affect the acid adenylation step vs. the amide bond forming step. The MSD trace (EIC with *m/z* of 236.1) is also included due to the low signal of procainamide under UV absorbance. Key: 'ML' is highest activity ML-predicted mutant, 'ISM' is a 'rational' design from combining the 4 highest activity single mutations from the HSS, and 'HSS' is the highest activity single mutant from the HSS. Data are representative of three independent experiments.

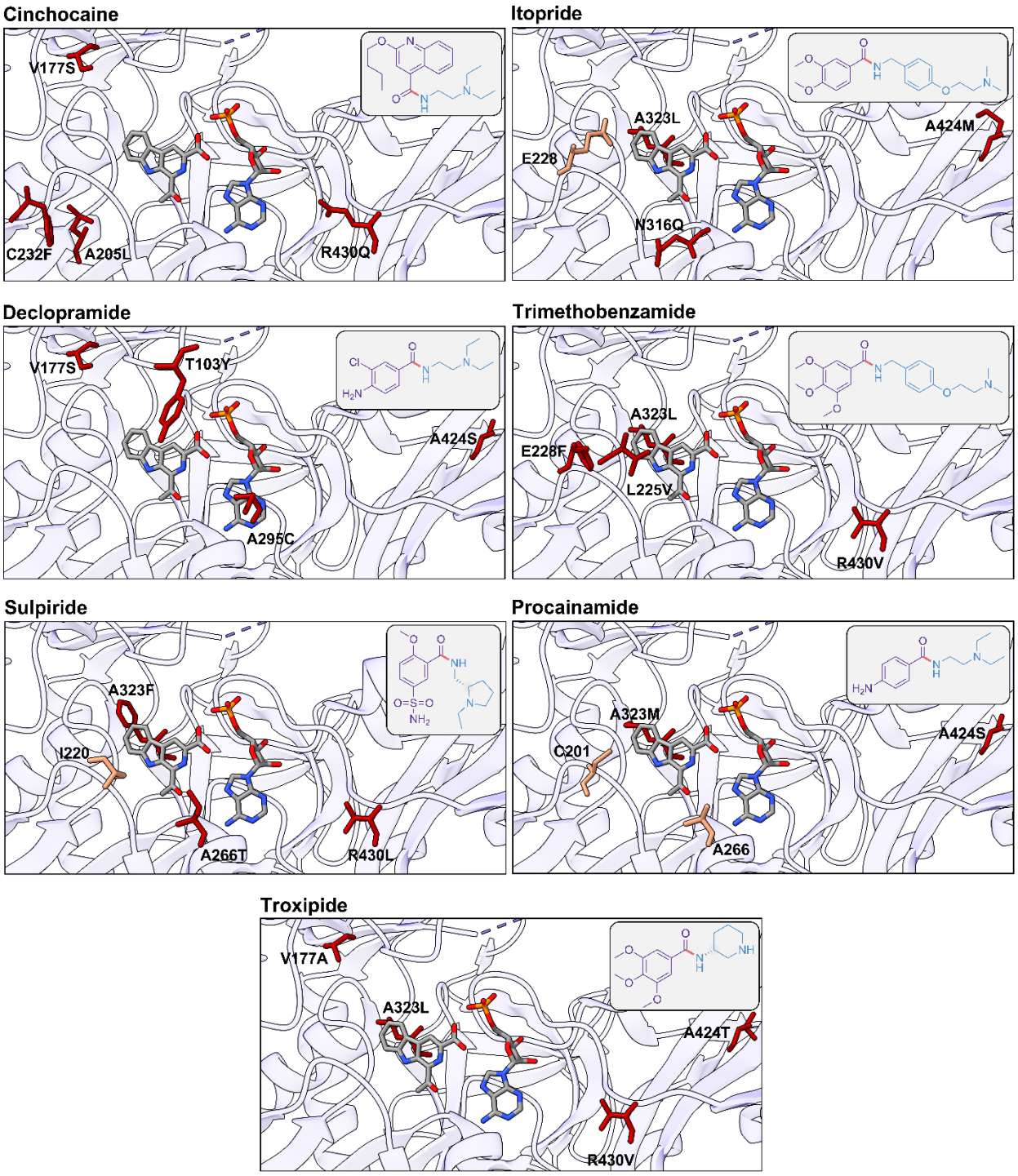

Figure S25. Modeling the active sites of the best ML-predicted mutations reveals trends in mutations for different substrates. We visualized the active site of different McbA mutants. We used the previously crystalized McbA (PDB: 6SQ8) as the backbone and left the native crystalized substrates in the active site. Amino acid changes were made at select residues using the rotamer tool with default parameters in ChimeraX.

Supplementary Tables

Table S1. Experimental validation of ML-predicted McbA mutants for moclobemide and metoclopramide. Variant ID corresponds to the four residues mutated for moclobemide (V177, I220, A323, R430) and metoclopramide (V177, T319, A323, A424), in the given order. Variants are rank ordered according to their experimentally measured yield via liquid chromatography (LC) with their predicted rank given. Amino acids colored red correspond to a residue containing the wild type (unmutated) amino acid. A negative control with sfGFP is also included. Reported yields are averages and standard deviations of $n = 3$ reactions.

Moclobemide			Metoclopramide		
Variant ID	Predicted Rank	% Conversion	Variant ID	Predicted Rank	% Conversion
SSFT	7	70.1 ± 0.3	SCFS	10	60.5 ± 1.1
SSFI	12	67.6 ± 0.7	SCFT	2	47.8 ± 0.3
SSFV	1	67.6 ± 0.3	SAFS	16	45.2 ± 0.4
SSFL	14	67.4 ± 0.2	SSFT	22	44.6 ± 2.3
SSFQ	5	66.3 ± 0.4	SCLT	12	27.4 ± 0.4
SSLC	16	65.4 ± 0.2	STFT	8	25.2 ± 1.0
SSFR	8	64.7 ± 0.9	SAFT	4	22.8 ± 3.5
SSLQ	11	63.2 ± 0.7	VCFT	5	17.8 ± 0.9
SSLT	18	63.2 ± 0.4	SLFT	20	13.8 ± 0.7
SSFC	6	63.1 ± 0.2	SEFT	19	9.07 ± 1.3
SSLV	2	62.6 ± 0.4	VAFT	6	8.65 ± 1.9
SSLI	25	61.4 ± 0.2	YSFT	18	6.97 ± 0.0
SSFN	9	60.6 ± 1.0	YCFS	9	4.57 ± 0.6
SSLN	22	58.3 ± 0.3	YCFT	1	3.63 ± 0.1
SSLR	21	57.6 ± 0.3	YCLT	11	2.85 ± 0.5
SAFV	17	56.0 ± 0.7	KCFT	24	2.17 ± 0.3
STFV	19	53.8 ± 0.1	YTFT	7	2.04 ± 1.3
SIFQ	24	50.6 ± 0.0	YAFS	15	0.22 ± 0.1
SIFV	4	50.1 ± 0.3	YLFT	21	0.09 ± 0.0
SSVV	3	47.1 ± 1.0	YEFT	17	0.09 ± 0.0
SILV	10	46.8 ± 0.5	SYFT	14	0.08 ± 0.0
SSVQ	15	39.5 ± 0.6	YMFT	25	0.08 ± 0.0
SIVV	13	26.8 ± 0.8	YYFT	13	0.05 ± 0.0
SSVT	23	22.8 ± 1.8	YKFT	23	0.03 ± 0.0
SSVC	20	20.5 ± 0.8	YAFT	3	0 ± 0
wt	-	4.38 ± 1.1	wt	-	1.37 ± 0.5
sfGFP	-	0 ± 0	sfGFP	-	0 ± 0

Table S2. Experimental validation of ML-predicted McbA mutants for cinchocaine. Variant ID corresponds to the four residues mutated for cinchocaine (V177, A205, C232, R430) in the given order. Variants are rank ordered according to their experimentally measured yield via LC with their predicted rank given. Amino acids colored red correspond to a residue containing the wild type (unmutated) amino acid. A negative control with sfGFP is also included. Reported yields are averages and standard deviations of n = 3 reactions.

Cinchocaine

Variant ID	Predicted Rank	% Conversion
SLFQ	11	4.9 ± 0.1
SCFV	20	4.5 ± 0.3
SSFQ	18	4.3 ± 0.0
SAFQ	10	4.2 ± 0.0
SLFV	6	3.7 ± 0.3
SAFV	7	3.6 ± 0.5
SAFT	22	3.1 ± 0.7
SSFV	14	3.0 ± 0.0
SMYQ	17	2.9 ± 0.1
STFV	23	2.8 ± 0.4
SMFV	1	2.6 ± 0.2
SMFN	4	2.6 ± 0.0
SMFT	3	2.5 ± 0.0
SLFT	21	2.5 ± 0.0
SMFQ	2	2.4 ± 0.0
SMFA	9	2.2 ± 0.0
SMYV	13	2.2 ± 0.0
SMFG	12	1.9 ± 0.1
SMFI	5	1.9 ± 0.1
SMFS	24	1.8 ± 0.4
SMFR	15	1.7 ± 0.0
SMFM	16	1.6 ± 0.0
SMFL	8	1.4 ± 0.1
SMQV	19	0.6 ± 0.0
WT	-	1.9 ± 0.1
sfGFP	-	0 ± 0

Table S3. Experimental validation of ML-predicted McbA mutants for itopride and declopramide. Variant ID corresponds to the four residues mutated for itopride (E228, N316, A323, A424) and declopramide (T103, V177, A295, A424) in the given order. Variants are rank ordered according to their experimentally measured extracted ion chromatogram (EIC; *m*/z of 359.2 and 270.1 for itopride and declopramide, respectively) with their predicted rank given. Amino acids colored red correspond to a residue containing the wild type (unmutated) amino acid. A negative control with sfGFP is also included. Reported EICs are averages plus or minus standard deviations of $n = 3$ reactions. EIC values were normalized by dividing EIC by the measured DAD (245 nm) peak area of the acid substrate. Here, we use these values qualitatively to identify the highest activity variant.

Itopride			Declopramide		
Variant ID	Predicted Rank	Normalized EIC	Variant ID	Predicted Rank	Normalized EIC
EQLM	11	159.3 ± 7.4	YSCS	24	1920 ± 209
EQLA	1	152.9 ± 46.3	YSRS	1	987.2 ± 45.7
LQLG	4	104.3 ± 1.2	YSMS	2	511.6 ± 23.2
QQLG	15	82.8 ± 2.0	YSQS	11	431.8 ± 23.7
IQLG	10	81.6 ± 0.7	WSRS	7	401.1 ± 33.4
LQLA	3	78.6 ± 1.0	WSMS	13	265.5 ± 6.4
TQLG	6	67.0 ± 14.	YVRS	5	246.8 ± 27.6
QQLA	9	66.6 ± 2.9	KSRS	17	179.6 ± 9.0
CQLG	24	58.8 ± 9.8	YVMS	10	171.9 ± 7.7
IQLA	7	58.6 ± 8.6	WSYS	22	169.6 ± 6.4
VQLA	19	56.4 ± 10.	LSRS	23	152.5 ± 7.3
FQLG	12	52.4 ± 0.6	YSHS	18	148.0 ± 9.0
TQLA	5	46.7 ± 8.2	YSFS	9	131.7 ± 8.6
HQLA	20	46.0 ± 6.1	NSRS	16	118.4 ± 9.4
FQLA	8	45.8 ± 1.4	YSYS	4	86.2 ± 6.8
YQLG	22	41.5 ± 3.8	YSES	19	79.6 ± 6.2
AQLA	13	40.3 ± 1.4	YSWS	8	73.8 ± 7.4
CQLA	18	36.2 ± 1.5	YSVS	3	66.5 ± 4.0
YQLA	14	33.2 ± 1.9	WSVS	21	64.7 ± 2.5
SQLA	17	32.8 ± 1.4	YYRS	14	63.8 ± 6.5
EQLG	2	32.6 ± 2.9	YVYS	15	46.7 ± 2.4
AQLG	21	31.4 ± 7.1	YSDS	6	40.9 ± 3.5
PQLG	23	22.4 ± 1.9	YSKS	20	40.2 ± 4.3
PQLA	16	17.4 ± 0.2	YVVS	12	23.6 ± 1.3
WT	-	2.6 ± 0.1	WT	-	271.7 ± 22.0
sfGFP	-	1.5 ± 0.0	sfGFP	-	1.9 ± 0.2

Table S4. Experimental validation of ML-predicted McbA mutants for trimethobenzamide and S-sulpiride. Variant ID corresponds to the four residues mutated for trimethobenzamide (L225, E228, A323, R430) and sulpiride (I220, A266, A323, R430) in the given order. Variants are rank ordered according to their experimentally measured EIC (*m*/z of 389.2 and 342.1 for trimethobenzamide and sulpiride, respectively) with their predicted rank given. Amino acids colored red correspond to a residue containing the wild type (unmutated) amino acid. A negative control with sfGFP is also included. Reported EICs are averages plus or minus standard deviations of $n = 3$ reactions. EIC values were normalized by dividing EIC by the measured DAD (245 nm) peak area of the acid substrate. Here, we use these values qualitatively to identify the highest activity variant.

Trimethobenzamide			Sulpiride		
Variant ID	Predicted Rank	Normalized EIC	Variant ID	Predicted Rank	Normalized EIC
VFLV	23	523.3 ± 12.8	ITFV	3	64.4 ± 4.0
VILV	18	384.5 ± 72.6	TTFV	20	64.1 ± 7.1
LELV	1	261.0 ± 27.9	STFV	21	59.4 ± 3.2
LELI	13	131.2 ± 7.3	ITFQ	8	52.4 ± 6.4
LELA	5	127.5 ± 6.3	ITFT	1	42.4 ± 2.0
LELT	6	124.9 ± 3.9	ITFA	19	32.7 ± 6.8
VELV	2	98.9 ± 2.2	STFT	7	30.4 ± 3.2
VILR	22	86.4 ± 1.0	TTFT	10	30.4 ± 2.9
VELT	8	78.2 ± 5.1	ITMV	16	24.3 ± 1.2
LQLV	17	73.7 ± 11.	ITMT	4	14.8 ± 0.4
VELA	7	67.7 ± 2.2	STMT	24	11.7 ± 2.6
VELI	11	65.0 ± 3.4	ITGT	6	4.0 ± 0.3
LILV	9	62.9 ± 8.2	ITLV	5	4.0 ± 0.9
LELR	4	39.7 ± 1.0	ITQT	23	3.3 ± 0.5
LALV	24	39.7 ± 2.0	STGT	22	3.2 ± 0.5
IELV	12	38.7 ± 1.5	ITAT	17	2.7 ± 0.3
LFLV	15	30.5 ± 1.8	ITLT	2	2.7 ± 0.5
VELR	3	26.1 ± 0.3	ITLA	18	2.6 ± 0.4
LILR	19	24.0 ± 2.9	ITLQ	11	2.5 ± 1.2
TELV	21	21.3 ± 0.4	TTLT	12	2.5 ± 0.4
LQLR	20	13.7 ± 0.7	STLT	9	2.2 ± 1.6
IELR	10	13.6 ± 0.4	ITTT	15	2.1 ± 0.5
SELV	14	4.18 ± 0.0	ITGV	13	1.8 ± 1.8
SELR	16	1.91 ± 0.0	ITVT	14	0.3 ± 0.4
WT	-	1.04 ± 0.0	WT	-	1.7 ± 0.3
sfGFP	-	0.79 ± 0.0	sfGFP	-	1.3 ± 0.1

Table S5. Experimental validation of predicted ML-McbA mutants for procainamide and troxipide. Variant ID corresponds to the four residues mutated for procainamide (C201, A266, A323, A424) and troxipide (V177, A323, A424, R430) in the given order. Variants are rank ordered according to their experimentally measured EIC (*m*/z of 236.1 and 295.1 for procainamide and troxipide, respectively) with their predicted rank given. Amino acids colored red correspond to a residue containing the wild type (unmutated) amino acid. A negative control with sfGFP is also included. Reported EICs are averages plus or minus standard deviations of $n = 3$ reactions. EIC values were normalized by dividing EIC by the measured DAD (245 nm) peak area of the acid substrate. Here, we use these values qualitatively to identify the highest activity variant.

Procainamide			Troxipide		
Variant ID	**Predicted Rank**	**Normalized EIC**	**Variant ID**	**Predicted Rank**	**Normalized EIC**
CAMS	24	6.3 ± 2.8	ALTV	16	4109 ± 221
CTMT	6	4.0 ± 0.5	SLTV	7	3293 ± 91
CTMS	2	2.5 ± 0.1	SLTA	23	2275 ± 127
STMS	1	2.4 ± 1.1	MLTV	17	1775 ± 137
CTMG	5	2.3 ± 0.1	VLTV	1	1742 ± 36
STMT	4	1.8 ± 0.0	VLTQ	9	1188 ± 25
STQS	22	1.6 ± 0.5	VLTT	4	1145 ± 17
CTFS	8	1.1 ± 0.4	SLTR	12	986 ± 27
CTLS	20	0.4 ± 0.6	VLTA	3	963 ± 19
STFS	7	0.4 ± 0.6	VLTI	5	840 ± 23
STMG	3	0.4 ± 0.6	VLTL	21	749 ± 34
SAMS	18	0.3 ± 0.5	VLTN	13	658 ± 53
STMA	9	0 ± 0	VLTS	11	600 ± 16
STFG	10	0 ± 0	VLTR	2	433 ± 17
CTMA	11	0 ± 0	LLTV	10	259 ± 9
STFT	12	0 ± 0	LLTA	24	229 ± 13
CTFG	13	0 ± 0	RLTV	6	65.4 ± 1.6
STYS	14	0 ± 0	VLAV	18	50.9 ± 5.4
CTFT	15	0 ± 0	LLTR	14	42.0 ± 2.6
STGS	16	0 ± 0	RLTT	19	27.8 ± 17.9
STLS	17	0 ± 0	RLTR	8	20.2 ± 0.6
CTGS	19	0 ± 0	VLGV	15	10.5 ± 0.8
STAS	21	0 ± 0	RLTA	20	10.3 ± 0.3
CTYS	23	0 ± 0	VLGR	22	4.9 ± 0.3
WT	-	0.7 ± 1.1	WT	-	2.8 ± 0.0
sfGFP	-	0 ± 0	sfGFP	-	2.2 ± 0.1

Table S6. Codon-optimized DNA sequences. Protein-encoding DNA sequences for McbA variants used in this study are shown below. We include wt-McbA, the two qm-McbA variants from our ISM engineering campaigns for moclobemide and metoclopramide, and the best experimentally validated ML-predicted variant for each compound (designated ml-McbA^{compound}). The Variant ID corresponding to **Table S1-5** is also included when available. For convenience, the N-terminal CSL-tag (containing a strep purification tag; see Methods) and TEV protease cleavage site on every variant is colored blue and the mutations made relative to wt-McbA are colored red. The amino acid labeling found in this work is based off these sequences (i.e., ATG = M1), which notably slightly deviates from previously published work and the crystal structure of McbA (PDB: 6SQ8) that does not include a CSL-tag.

Enzyme	Sequence
wt-McbA	ATGGAGAAAAAAATCTGGAGCCATCCGCAGTTCGAAAAAGGCGGATCCGG AGAAAACCTGTATTTCCAGGGCGGTTACGCTCGTCGTGTAATGGATGGTAT CGGTGAAGTAGCGGTAACTGGCGCTGGTGGTTCTGTAACTGGTGCGCGTC TGCGCCATCAGGTTCGTCTGCTGGCTCATGCTCTGACCGAAGCGGGTATT CCGCCAGGCCGTGGTGTAGCATGTCTGCATGCTAACACCTGGCGTGCGAT CGCACTGCGTCTGGCTGTTCAGGCGATTGGTTGCCACTATGTTGGTCTGC GTCCTACCGCTGCTGTTACTGAACAGGCACGCGCAATTGCGGCTGCTGAT TCTGCCGCACTGGTTTTCGAACCAAGCGTTGAAGCTCGTGCAGCTGACCT GCTGGAACGTGTTTCTGTGCCGGTTGTGCTGTCTCTGGGTCCGACCTCTC GTGGCCGTGATATCCTGGCAGCTAGCGTTCCGGAAGGTACGCCGCTGCG TTACCGTGAACACCCAGAAGGTATCGCAGTTGTAGCCTTTACTAGCGGCAC CACTGGCACCCCTAAAGGCGTTGCCCACTCCTCTACCGCTATGAGCGCTT GTGTGGATGCTGCGGTTTCCATGTACGGTCGCGGTCCTTGGCGTTTCCTG ATCCCGATCCCTCTGTCTGACCTGGGTGGCGAACTGGCACAGTGTACCCT GGCTACCGGCGGTACCGTTGTGCTGCTGGAAGAGTTCCAACCGGACGCC GTTCTGGAAGCTATCGAACGTGAACGTGCCACTCACGTGTTCCTGGCGCC GAACTGGCTGTACCAGCTGGCTGAACATCCGGCTCTGCCGCGTTCTGATC TGTCTTCTCTGCGTCGCGTTGTTTACGGCGGTGCACCGGCAGTACCATCT CGTGTAGCAGCAGCACGTGAACGTATGGGTGCTGTGCTGATGCAGAACTA CGGCACCCAGGAAGCAGCTTTCATCGCAGCACTGACTCCAGACGATCACG CACGTCGTGAACTGCTGACCGCTGTAGGTCGTCCTCTGCCACACGTTGAG GTGGAAATCCGTGATGACTCTGGTGGTACTCTGCCGCGTGGTGCGGTAGG TGAAGTCTGGGTACGTTCCCCGATGACTATGTCTGGTTACTGGCGTGACC CGGAACGTACGGCTCAGGTTCTGTCTGGTGGTTGGCTGCGTACTGGTGAT GTTGGTACCTTCGATGAGGATGGTCACCTGCATCTGACCGATCGTCTGCA GGACATCATCATCGTTGAAGCATATAACGTCTATTCCCGTCGTGTGGAACA TGTTCTGACCGAACACCCAGATGTTCGCGCAGCTGCGGTTGTTGGCGTAC CAGATCCGGACTCTGGTGAAGCTGTTTGCGCTGCGGTTGTAGTCGCGGAT GGTGCGGATCCTGACCCTGAACACCTGCGTGCTCTGGTTCGTGATCACCT GGGTGATCTGCACGTTCCTCGCCGTGTTGAGTTCGTTCGCTCCATCCCGG TAACTCCTGCCGGCAAACCAGATAAAGTGAAAGTGCGTACCTGGTTCACC GACTAA
qm-McbA$_{moclobemide}$	ATGGAGAAAAAAATCTGGAGCCATCCGCAGTTCGAAAAAGGCGGATCCGG AGAAAACCTGTATTTCCAGGGCGGTTACGCTCGTCGTGTAATGGATGGTAT CGGTGAAGTAGCGGTAACTGGCGCTGGTGGTTCTGTAACTGGTGCGCGTC TGCGCCATCAGGTTCGTCTGCTGGCTCATGCTCTGACCGAAGCGGGTATT CCGCCAGGCCGTGGTGTAGCATGTCTGCATGCTAACACCTGGCGTGCGAT

	CGCACTGCGTCTGGCTGTTCAGGCGATTGGTTGCCACTATGTTGGTCTGC GTCCTACCGCTGCTGTTACTGAACAGGCACGCGCAATTGCGGCTGCTGAT TCTGCCGCACTGGTTTTCGAACCAAGCGTTGAAGCTCGTGCAGCTGACCT GCTGGAACGTGTTTCTGTGCCGGTTGTGCTGTCTCTGGGTCCGACCTCTC GTGGCCGTGATATCCTGGCAGCTAGCGTTCCGGAAGGTACGCCGCTGCG TTACCGTGAACACCCAGAAGGTATCGCAAGCGTAGCCTTTACTAGCGGCA CCACTGGCACCCCTAAAGGCGTTGCCCACTCCTCTACCGCTATGAGCGCT TGTGTGGATGCTGCGGTTTCCATGTACGGTCGCGGTCCTTGGCGTTTCCT GATCCCGAGCCCTCTGTCTGACCTGGGTGGCGAACTGGCACAGTGTACCC TGGCTACCGGCGGTACCGTTGTGCTGCTGGAAGAGTTCCAACCGGACGC CGTTCTGGAAGCTATCGAACGTGAACGTGCCACTCACGTGTTCCTGGCGC CGAACTGGCTGTACCAGCTGGCTGAACATCCGGCTCTGCCGCGTTCTGAT CTGTCTTCTCTGCGTCGCGTTGTTTACGGCGGTGCACCGGCAGTACCATC TCGTGTAGCAGCAGCACGTGAACGTATGGGTGCTGTGCTGATGCAGAACT ACGGCACCCAGGAAGCATTTTTCATCGCAGCACTGACTCCAGACGATCAC GCACGTCGTGAACTGCTGACCGCTGTAGGTCGTCCTCTGCCACACGTTGA GGTGGAAATCCGTGATGACTCTGGTGGTACTCTGCCGCGTGGTGCGGTAG GTGAAGTCTGGGTACGTTCCCCGATGACTATGTCTGGTTACTGGCGTGAC CCGGAACGTACGGCTCAGGTTCTGTCTGGTGGTTGGCTGCGTACTGGTGA TGTTGGTACCTTCGATGAGGATGGTCACCTGCATCTGACCGATCGTCTGCA GGACATCATCATCGTTGAAGCATATAACGTCTATTCCCTGCGTGTGGAACA TGTTCTGACCGAACACCCAGATGTTCGCGCAGCTGCGGTTGTTGGCGTAC CAGATCCGGACTCTGGTGAAGCTGTTTGCGCTGCGGTTGTAGTCGCGGAT GGTGCGGATCCTGACCCTGAACACCTGCGTGCTCTGGTTCGTGATCACCT GGGTGATCTGCACGTTCCTCGCCGTGTTGAGTTCGTTCGCTCCATCCCGG TAACTCCTGCCGGCAAACCAGATAAAGTGAAAGTGCGTACCTGGTTCACC GACTAA
qm-McbA$_{metoclopramide}$	ATGGAGAAAAAAATCTGGAGCCATCCGCAGTTCGAAAAAGGCGGATCCGG AGAAAACCTGTATTTCCAGGGCGGTTACGCTCGTCGTGTAATGGATGGTAT CGGTGAAGTAGCGGTAACTGGCGCTGGTGGTTCTGTAACTGGTGCGCGTC TGCGCCATCAGGTTCGTCTGCTGGCTCATGCTCTGACCGAAGCGGGTATT CCGCCAGGCCGTGGTGTAGCATGTCTGCATGCTAACACCTGGCGTGCGAT CGCACTGCGTCTGGCTGTTCAGGCGATTGGTTGCCACTATGTTGGTCTGC GTCCTACCGCTGCTGTTACTGAACAGGCACGCGCAATTGCGGCTGCTGAT TCTGCCGCACTGGTTTTCGAACCAAGCGTTGAAGCTCGTGCAGCTGACCT GCTGGAACGTGTTTCTGTGCCGGTTGTGCTGTCTCTGGGTCCGACCTCTC GTGGCCGTGATATCCTGGCAGCTAGCGTTCCGGAAGGTACGCCGCTGCG TTACCGTGAACACCCAGAAGGTATCGCAAGCGTAGCCTTTACTAGCGGCA CCACTGGCACCCCTAAAGGCGTTGCCCACTCCTCTACCGCTATGAGCGCT TGTGTGGATGCTGCGGTTTCCATGTACGGTCGCGGTCCTTGGCGTTTCCT GATCCCGATCCCTCTGTCTGACCTGGGTGGCGAACTGGCACAGTGTACCC TGGCTACCGGCGGTACCGTTGTGCTGCTGGAAGAGTTCCAACCGGACGC CGTTCTGGAAGCTATCGAACGTGAACGTGCCACTCACGTGTTCCTGGCGC CGAACTGGCTGTACCAGCTGGCTGAACATCCGGCTCTGCCGCGTTCTGAT CTGTCTTCTCTGCGTCGCGTTGTTTACGGCGGTGCACCGGCAGTACCATC TCGTGTAGCAGCAGCACGTGAACGTATGGGTGCTGTGCTGATGCAGAACT ACGGCTGCCAGGAAGCATTTTTCATCGCAGCACTGACTCCAGACGATCAC GCACGTCGTGAACTGCTGACCGCTGTAGGTCGTCCTCTGCCACACGTTGA GGTGGAAATCCGTGATGACTCTGGTGGTACTCTGCCGCGTGGTGCGGTAG GTGAAGTCTGGGTACGTTCCCCGATGACTATGTCTGGTTACTGGCGTGAC CCGGAACGTACGGCTCAGGTTCTGTCTGGTGGTTGGCTGCGTACTGGTGA

	TGTTGGTACCTTCGATGAGGATGGTCACCTGCATCTGACCGATCGTCTGCA GGACATCATCATCGTTGAAACCTATAACGTCTATTCCCGTCGTGTGGAACA TGTTCTGACCGAACACCCAGATGTTCGCGCAGCTGCGGTTGTTGGCGTAC CAGATCCGGACTCTGGTGAAGCTGTTTGCGCTGCGGTTGTAGTCGCGGAT GGTGCGGATCCTGACCCTGAACACCTGCGTGCTCTGGTTCGTGATCACCT GGGTGATCTGCACGTTCCTCGCCGTGTTGAGTTCGTTCGCTCCATCCCGG TAACTCCTGCCGGCAAACCAGATAAAGTGAAAGTGCGTACCTGGTTCACC GACTAA
ml-McbA$_{moclobemide}$ (SSFT)	ATGGAGAAAAAAATCTGGAGCCATCCGCAGTTCGAAAAAGGCGGATCCGG AGAAAACCTGTATTTCCAGGGCGGTTACGCTCGTCGTGTAATGGATGGTAT CGGTGAAGTAGCGGTAACTGGCGCTGGTGGTTCTGTAACTGGTGCGCGTC TGCGCCATCAGGTTCGTCTGCTGGCTCATGCTCTGACCGAAGCGGGTATT CCGCCAGGCCGTGGTGTAGCATGTCTGCATGCTAACACCTGGCGTGCGAT CGCACTGCGTCTGGCTGTTCAGGCGATTGGTTGCCACTATGTTGGTCTGC GTCCTACCGCTGCTGTTACTGAACAGGCACGCGCAATTGCGGCTGCTGAT TCTGCCGCACTGGTTTTCGAACCAAGCGTTGAAGCTCGTGCAGCTGACCT GCTGGAACGTGTTTCTGTGCCGGTTGTGCTGTCTCTGGGTCCGACCTCTC GTGGCCGTGATATCCTGGCAGCTAGCGTTCCGGAAGGTACGCCGCTGCG TTACCGTGAACACCCAGAAGGTATCGCAAGCGTAGCCTTTACTAGCGGCA CCACTGGCACCCCTAAAGGCGTTGCCCACTCCTCTACCGCTATGAGCGCT TGTGTGGATGCTGCGGTTTCCATGTACGGTCGCGGTCCTTGGCGTTTCCT GATCCCGAGCCCTCTGTCTGACCTGGGTGGCGAACTGGCACAGTGTACCC TGGCTACCGGCGGTACCGTTGTGCTGCTGGAAGAGTTCCAACCGGACGC CGTTCTGGAAGCTATCGAACGTGAACGTGCCACTCACGTGTTCCTGGCGC CGAACTGGCTGTACCAGCTGGCTGAACATCCGGCTCTGCCGCGTTCTGAT CTGTCTTCTCTGCGTCGCGTTGTTTACGGCGGTGCACCGGCAGTACCATC TCGTGTAGCAGCAGCACGTGAACGTATGGGTGCTGTGCTGATGCAGAACT ACGGCACCCAGGAAGCATTTTTCATCGCAGCACTGACTCCAGACGATCAC GCACGTCGTGAACTGCTGACCGCTGTAGGTCGTCCTCTGCCACACGTTGA GGTGGAAATCCGTGATGACTCTGGTGGTACTCTGCCGCGTGGTGCGGTAG GTGAAGTCTGGGTACGTTCCCCGATGACTATGTCTGGTTACTGGCGTGAC CCGGAACGTACGGCTCAGGTTCTGTCTGGTGGTTGGCTGCGTACTGGTGA TGTTGGTACCTTCGATGAGGATGGTCACCTGCATCTGACCGATCGTCTGCA GGACATCATCATCGTTGAAGCATATAACGTCTATTCCACCCGTGTGGAACA TGTTCTGACCGAACACCCAGATGTTCGCGCAGCTGCGGTTGTTGGCGTAC CAGATCCGGACTCTGGTGAAGCTGTTTGCGCTGCGGTTGTAGTCGCGGAT GGTGCGGATCCTGACCCTGAACACCTGCGTGCTCTGGTTCGTGATCACCT GGGTGATCTGCACGTTCCTCGCCGTGTTGAGTTCGTTCGCTCCATCCCGG TAACTCCTGCCGGCAAACCAGATAAAGTGAAAGTGCGTACCTGGTTCACC GACTAA
ml-McbA$_{metoclopramide}$ (SCFS)	ATGGAGAAAAAAATCTGGAGCCATCCGCAGTTCGAAAAAGGCGGATCCGG AGAAAACCTGTATTTCCAGGGCGGTTACGCTCGTCGTGTAATGGATGGTAT CGGTGAAGTAGCGGTAACTGGCGCTGGTGGTTCTGTAACTGGTGCGCGTC TGCGCCATCAGGTTCGTCTGCTGGCTCATGCTCTGACCGAAGCGGGTATT CCGCCAGGCCGTGGTGTAGCATGTCTGCATGCTAACACCTGGCGTGCGAT CGCACTGCGTCTGGCTGTTCAGGCGATTGGTTGCCACTATGTTGGTCTGC GTCCTACCGCTGCTGTTACTGAACAGGCACGCGCAATTGCGGCTGCTGAT TCTGCCGCACTGGTTTTCGAACCAAGCGTTGAAGCTCGTGCAGCTGACCT GCTGGAACGTGTTTCTGTGCCGGTTGTGCTGTCTCTGGGTCCGACCTCTC GTGGCCGTGATATCCTGGCAGCTAGCGTTCCGGAAGGTACGCCGCTGCG TTACCGTGAACACCCAGAAGGTATCGCAAGCGTAGCCTTTACTAGCGGCA CCACTGGCACCCCTAAAGGCGTTGCCCACTCCTCTACCGCTATGAGCGCT

	TGTGTGGATGCTGCGGTTTCCATGTACGGTCGCGGTCCTTGGCGTTTCCT GATCCCGATCCCTCTGTCTGACCTGGGTGGCGAACTGGCACAGTGTACCC TGGCTACCGGCGGTACCGTTGTGCTGCTGGAAGAGTTCCAACCGGACGC CGTTCTGGAAGCTATCGAACGTGAACGTGCCACTCACGTGTTCCTGGCGC CGAACTGGCTGTACCAGCTGGCTGAACATCCGGCTCTGCCGCGTTCTGAT CTGTCTTCTCTGCGTCGCGTTGTTTACGGCGGTGCACCGGCAGTACCATC TCGTGTAGCAGCAGCACGTGAACGTATGGGTGCTGTGCTGATGCAGAACT ACGGCTGCCAGGAAGCATTTTTCATCGCAGCACTGACTCCAGACGATCAC GCACGTCGTGAACTGCTGACCGCTGTAGGTCGTCCTCTGCCACACGTTGA GGTGGAAATCCGTGATGACTCTGGTGGTACTCTGCCGCGTGGTGCGGTAG GTGAAGTCTGGGTACGTTCCCCGATGACTATGTCTGGTTACTGGCGTGAC CCGGAACGTACGGCTCAGGTTCTGTCTGGTGGTTGGCTGCGTACTGGTGA TGTTGGTACCTTCGATGAGGATGGTCACCTGCATCTGACCGATCGTCTGCA GGACATCATCATCGTTGAAAGCTATAACGTCTATTCCCGTCGTGTGGAACA TGTTCTGACCGAACACCCAGATGTTCGCGCAGCTGCGGTTGTTGGCGTAC CAGATCCGGACTCTGGTGAAGCTGTTTGCGCTGCGGTTGTAGTCGCGGAT GGTGCGGATCCTGACCCTGAACACCTGCGTGCTCTGGTTCGTGATCACCT GGGTGATCTGCACGTTCCTCGCCGTGTTGAGTTCGTTCGCTCCATCCCGG TAACTCCTGCCGGCAAACCAGATAAAGTGAAAGTGCGTACCTGGTTCACC GACTAA
ml-McbA$_{cinchocaine}$ (SLFQ)	ATGGAGAAAAAAATCTGGAGCCATCCGCAGTTCGAAAAAGGCGGATCCGG AGAAAACCTGTATTTCCAGGGCGGTTACGCTCGTCGTGTAATGGATGGTAT CGGTGAAGTAGCGGTAACTGGCGCTGGTGGTTCTGTAACTGGTGCGCGTC TGCGCCATCAGGTTCGTCTGCTGGCTCATGCTCTGACCGAAGCGGGTATT CCGCCAGGCCGTGGTGTAGCATGTCTGCATGCTAACACCTGGCGTGCGAT CGCACTGCGTCTGGCTGTTCAGGCGATTGGTTGCCACTATGTTGGTCTGC GTCCTACCGCTGCTGTTACTGAACAGGCACGCGCAATTGCGGCTGCTGAT TCTGCCGCACTGGTTTTCGAACCAAGCGTTGAAGCTCGTGCAGCTGACCT GCTGGAACGTGTTTCTGTGCCGGTTGTGCTGTCTCTGGGTCCGACCTCTC GTGGCCGTGATATCCTGGCAGCTAGCGTTCCGGAAGGTACGCCGCTGCG TTACCGTGAACACCCAGAAGGTATCGCAAGCGTAGCCTTTACTAGCGGCA CCACTGGCACCCCTAAAGGCGTTGCCCACTCCTCTACCGCTATGAGCGCT TGTGTGGATGCTCTGGTTTCCATGTACGGTCGCGGTCCTTGGCGTTTCCT GATCCCGATCCCTCTGTCTGACCTGGGTGGCGAACTGGCACAGTTTACCC TGGCTACCGGCGGTACCGTTGTGCTGCTGGAAGAGTTCCAACCGGACGC CGTTCTGGAAGCTATCGAACGTGAACGTGCCACTCACGTGTTCCTGGCGC CGAACTGGCTGTACCAGCTGGCTGAACATCCGGCTCTGCCGCGTTCTGAT CTGTCTTCTCTGCGTCGCGTTGTTTACGGCGGTGCACCGGCAGTACCATC TCGTGTAGCAGCAGCACGTGAACGTATGGGTGCTGTGCTGATGCAGAACT ACGGCACCCAGGAAGCAGCTTTCATCGCAGCACTGACTCCAGACGATCAC GCACGTCGTGAACTGCTGACCGCTGTAGGTCGTCCTCTGCCACACGTTGA GGTGGAAATCCGTGATGACTCTGGTGGTACTCTGCCGCGTGGTGCGGTAG GTGAAGTCTGGGTACGTTCCCCGATGACTATGTCTGGTTACTGGCGTGAC CCGGAACGTACGGCTCAGGTTCTGTCTGGTGGTTGGCTGCGTACTGGTGA TGTTGGTACCTTCGATGAGGATGGTCACCTGCATCTGACCGATCGTCTGCA GGACATCATCATCGTTGAAGCATATAACGTCTATTCCCAGCGTGTGGAACA TGTTCTGACCGAACACCCAGATGTTCGCGCAGCTGCGGTTGTTGGCGTAC CAGATCCGGACTCTGGTGAAGCTGTTTGCGCTGCGGTTGTAGTCGCGGAT GGTGCGGATCCTGACCCTGAACACCTGCGTGCTCTGGTTCGTGATCACCT GGGTGATCTGCACGTTCCTCGCCGTGTTGAGTTCGTTCGCTCCATCCCGG TAACTCCTGCCGGCAAACCAGATAAAGTGAAAGTGCGTACCTGGTTCACC GACTAA

ml-McbA$_{itopride}$ (EQLM)	ATGGAGAAAAAAATCTGGAGCCATCCGCAGTTCGAAAAAGGCGGATCCGG AGAAAACCTGTATTTCCAGGGCGGTTACGCTCGTCGTGTAATGGATGGTAT CGGTGAAGTAGCGGTAACTGGCGCTGGTGGTTCTGTAACTGGTGCGCGTC TGCGCCATCAGGTTCGTCTGCTGGCTCATGCTCTGACCGAAGCGGGTATT CCGCCAGGCCGTGGTGTAGCATGTCTGCATGCTAACACCTGGCGTGCGAT CGCACTGCGTCTGGCTGTTCAGGCGATTGGTTGCCACTATGTTGGTCTGC GTCCTACCGCTGCTGTTACTGAACAGGCACGCGCAATTGCGGCTGCTGAT TCTGCCGCACTGGTTTTCGAACCAAGCGTTGAAGCTCGTGCAGCTGACCT GCTGGAACGTGTTTCTGTGCCGGTTGTGCTGTCTCTGGGTCCGACCTCTC GTGGCCGTGATATCCTGGCAGCTAGCGTTCCGGAAGGTACGCCGCTGCG TTACCGTGAACACCCAGAAGGTATCGCAGTTGTAGCCTTTACTAGCGGCAC CACTGGCACCCCTAAAGGCGTTGCCCACTCCTCTACCGCTATGAGCGCTT GTGTGGATGCTGCGGTTTCCATGTACGGTCGCGGTCCTTGGCGTTTCCTG ATCCCGATCCCTCTGTCTGACCTGGGTGGCGAACTGGCACAGTGTACCCT GGCTACCGGCGGTACCGTTGTGCTGCTGGAAGAGTTCCAACCGGACGCC GTTCTGGAAGCTATCGAACGTGAACGTGCCACTCACGTGTTCCTGGCGCC GAACTGGCTGTACCAGCTGGCTGAACATCCGGCTCTGCCGCGTTCTGATC TGTCTTCTCTGCGTCGCGTTGTTTACGGCGGTGCACCGGCAGTACCATCT CGTGTAGCAGCAGCACGTGAACGTATGGGTGCTGTGCTGATGCAGCAGTA CGGCACCCAGGAAGCACTGTTCATCGCAGCACTGACTCCAGACGATCACG CACGTCGTGAACTGCTGACCGCTGTAGGTCGTCCTCTGCCACACGTTGAG GTGGAAATCCGTGATGACTCTGGTGGTACTCTGCCGCGTGGTGCGGTAGG TGAAGTCTGGGTACGTTCCCCGATGACTATGTCTGGTTACTGGCGTGACC CGGAACGTACGGCTCAGGTTCTGTCTGGTGGTTGGCTGCGTACTGGTGAT GTTGGTACCTTCGATGAGGATGGTCACCTGCATCTGACCGATCGTCTGCA GGACATCATCATCGTTGAAATGTATAACGTCTATTCCCGTCGTGTGGAACA TGTTCTGACCGAACACCCAGATGTTCGCGCAGCTGCGGTTGTTGGCGTAC CAGATCCGGACTCTGGTGAAGCTGTTTGCGCTGCGGTTGTAGTCGCGGAT GGTGCGGATCCTGACCCTGAACACCTGCGTGCTCTGGTTCGTGATCACCT GGGTGATCTGCACGTTCCTCGCCGTGTTGAGTTCGTTCGCTCCATCCCGG TAACTCCTGCCGGCAAACCAGATAAAGTGAAAGTGCGTACCTGGTTCACC GACTAA
ml-McbA$_{declopramide}$ (YSCS)	ATGGAGAAAAAAATCTGGAGCCATCCGCAGTTCGAAAAAGGCGGATCCGG AGAAAACCTGTATTTCCAGGGCGGTTACGCTCGTCGTGTAATGGATGGTAT CGGTGAAGTAGCGGTAACTGGCGCTGGTGGTTCTGTAACTGGTGCGCGTC TGCGCCATCAGGTTCGTCTGCTGGCTCATGCTCTGACCGAAGCGGGTATT CCGCCAGGCCGTGGTGTAGCATGTCTGCATGCTAACACCTGGCGTGCGAT CGCACTGCGTCTGGCTGTTCAGGCGATTGGTTGCCACTATGTTGGTCTGC GTCCTTATGCTGCTGTTACTGAACAGGCACGCGCAATTGCGGCTGCTGATT CTGCCGCACTGGTTTTCGAACCAAGCGTTGAAGCTCGTGCAGCTGACCTG CTGGAACGTGTTTCTGTGCCGGTTGTGCTGTCTCTGGGTCCGACCTCTCG TGGCCGTGATATCCTGGCAGCTAGCGTTCCGGAAGGTACGCCGCTGCGTT ACCGTGAACACCCAGAAGGTATCGCAAGCGTAGCCTTTACTAGCGGCACC ACTGGCACCCCTAAAGGCGTTGCCCACTCCTCTACCGCTATGAGCGCTTG TGTGGATGCTGCGGTTTCCATGTACGGTCGCGGTCCTTGGCGTTTCCTGA TCCCGATCCCTCTGTCTGACCTGGGTGGCGAACTGGCACAGTGTACCCTG GCTACCGGCGGTACCGTTGTGCTGCTGGAAGAGTTCCAACCGGACGCCG TTCTGGAAGCTATCGAACGTGAACGTGCCACTCACGTGTTCCTGGCGCCG AACTGGCTGTACCAGCTGGCTGAACATCCGGCTCTGCCGCGTTCTGATCT GTCTTCTCTGCGTCGCGTTGTTTACGGCGGTTGCCCGGCAGTACCATCTC GTGTAGCAGCAGCACGTGAACGTATGGGTGCTGTGCTGATGCAGAACTAC GGCACCCAGGAAGCAGCTTTCATCGCAGCACTGACTCCAGACGATCACGC

	ACGTCGTGAACTGCTGACCGCTGTAGGTCGTCCTCTGCCACACGTTGAGG TGGAAATCCGTGATGACTCTGGTGGTACTCTGCCGCGTGGTGCGGTAGGT GAAGTCTGGGTACGTTCCCCGATGACTATGTCTGGTTACTGGCGTGACCC GGAACGTACGGCTCAGGTTCTGTCTGGTGGTTGGCTGCGTACTGGTGATG TTGGTACCTTCGATGAGGATGGTCACCTGCATCTGACCGATCGTCTGCAG GACATCATCATCGTTGAAAGCTATAACGTCTATTCCCGTCGTGTGGAACAT GTTCTGACCGAACACCCAGATGTTCGCGCAGCTGCGGTTGTTGGCGTACC AGATCCGGACTCTGGTGAAGCTGTTTGCGCTGCGGTTGTAGTCGCGGATG GTGCGGATCCTGACCCTGAACACCTGCGTGCTCTGGTTCGTGATCACCTG GGTGATCTGCACGTTCCTCGCCGTGTTGAGTTCGTTCGCTCCATCCCGGT AACTCCTGCCGGCAAACCAGATAAAGTGAAAGTGCGTACCTGGTTCACCG ACTAA
ml-McbA$_{trimethobenzamide}$ (VFLV)	ATGGAGAAAAAAATCTGGAGCCATCCGCAGTTCGAAAAAGGCGGATCCGG AGAAAACCTGTATTTCCAGGGCGGTTACGCTCGTCGTGTAATGGATGGTAT CGGTGAAGTAGCGGTAACTGGCGCTGGTGGTTCTGTAACTGGTGCGCGTC TGCGCCATCAGGTTCGTCTGCTGGCTCATGCTCTGACCGAAGCGGGTATT CCGCCAGGCCGTGGTGTAGCATGTCTGCATGCTAACACCTGGCGTGCGAT CGCACTGCGTCTGGCTGTTCAGGCGATTGGTTGCCACTATGTTGGTCTGC GTCCTACCGCTGCTGTTACTGAACAGGCACGCGCAATTGCGGCTGCTGAT TCTGCCGCACTGGTTTTCGAACCAAGCGTTGAAGCTCGTGCAGCTGACCT GCTGGAACGTGTTTCTGTGCCGGTTGTGCTGTCTCTGGGTCCGACCTCTC GTGGCCGTGATATCCTGGCAGCTAGCGTTCCGGAAGGTACGCCGCTGCG TTACCGTGAACACCCAGAAGGTATCGCAGTTGTAGCCTTTACTAGCGGCAC CACTGGCACCCCTAAAGGCGTTGCCCACTCCTCTACCGCTATGAGCGCTT GTGTGGATGCTGCGGTTTCCATGTACGGTCGCGGTCCTTGGCGTTTCCTG ATCCCGATCCCTCTGTCTGACGTGGGTGGCTTTCTGGCACAGTGTACCCT GGCTACCGGCGGTACCGTTGTGCTGCTGGAAGAGTTCCAACCGGACGCC GTTCTGGAAGCTATCGAACGTGAACGTGCCACTCACGTGTTCCTGGCGCC GAACTGGCTGTACCAGCTGGCTGAACATCCGGCTCTGCCGCGTTCTGATC TGTCTTCTCTGCGTCGCGTTGTTTACGGCGGTGCACCGGCAGTACCATCT CGTGTAGCAGCAGCACGTGAACGTATGGGTGCTGTGCTGATGCAGAACTA CGGCACCCAGGAAGCACTGTTCATCGCAGCACTGACTCCAGACGATCACG CACGTCGTGAACTGCTGACCGCTGTAGGTCGTCCTCTGCCACACGTTGAG GTGGAAATCCGTGATGACTCTGGTGGTACTCTGCCGCGTGGTGCGGTAGG TGAAGTCTGGGTACGTTCCCCGATGACTATGTCTGGTTACTGGCGTGACC CGGAACGTACGGCTCAGGTTCTGTCTGGTGGTTGGCTGCGTACTGGTGAT GTTGGTACCTTCGATGAGGATGGTCACCTGCATCTGACCGATCGTCTGCA GGACATCATCATCGTTGAAGCATATAACGTCTATTCCGTGCGTGTGGAACA TGTTCTGACCGAACACCCAGATGTTCGCGCAGCTGCGGTTGTTGGCGTAC CAGATCCGGACTCTGGTGAAGCTGTTTGCGCTGCGGTTGTAGTCGCGGAT GGTGCGGATCCTGACCCTGAACACCTGCGTGCTCTGGTTCGTGATCACCT GGGTGATCTGCACGTTCCTCGCCGTGTTGAGTTCGTTCGCTCCATCCCGG TAACTCCTGCCGGCAAACCAGATAAAGTGAAAGTGCGTACCTGGTTCACC GACTAA
ml-McbA$_{sulpiride}$ (ITFV)	ATGGAGAAAAAAATCTGGAGCCATCCGCAGTTCGAAAAAGGCGGATCCGG AGAAAACCTGTATTTCCAGGGCGGTTACGCTCGTCGTGTAATGGATGGTAT CGGTGAAGTAGCGGTAACTGGCGCTGGTGGTTCTGTAACTGGTGCGCGTC TGCGCCATCAGGTTCGTCTGCTGGCTCATGCTCTGACCGAAGCGGGTATT CCGCCAGGCCGTGGTGTAGCATGTCTGCATGCTAACACCTGGCGTGCGAT CGCACTGCGTCTGGCTGTTCAGGCGATTGGTTGCCACTATGTTGGTCTGC GTCCTACCGCTGCTGTTACTGAACAGGCACGCGCAATTGCGGCTGCTGAT TCTGCCGCACTGGTTTTCGAACCAAGCGTTGAAGCTCGTGCAGCTGACCT

	GCTGGAACGTGTTTCTGTGCCGGTTGTGCTGTCTCTGGGTCCGACCTCTC GTGGCCGTGATATCCTGGCAGCTAGCGTTCCGGAAGGTACGCCGCTGCG TTACCGTGAACACCCAGAAGGTATCGCAGTTGTAGCCTTTACTAGCGGCAC CACTGGCACCCCTAAAGGCGTTGCCCACTCCTCTACCGCTATGAGCGCTT GTGTGGATGCTGCGGTTTCCATGTACGGTCGCGGTCCTTGGCGTTTCCTG ATCCCGATCCCTCTGTCTGACCTGGGTGGCGAACTGGCACAGTGTACCCT GGCTACCGGCGGTACCGTTGTGCTGCTGGAAGAGTTCCAACCGGACGCC GTTCTGGAAGCTATCGAACGTGAACGTGCCACTCACGTGTTCCTGACCCC GAACTGGCTGTACCAGCTGGCTGAACATCCGGCTCTGCCGCGTTCTGATC TGTCTTCTCTGCGTCGCGTTGTTTACGGCGGTGCACCGGCAGTACCATCT CGTGTAGCAGCAGCACGTGAACGTATGGGTGCTGTGCTGATGCAGAACTA CGGCACCCAGGAAGCATTTTTCATCGCAGCACTGACTCCAGACGATCACG CACGTCGTGAACTGCTGACCGCTGTAGGTCGTCCTCTGCCACACGTTGAG GTGGAAATCCGTGATGACTCTGGTGGTACTCTGCCGCGTGGTGCGGTAGG TGAAGTCTGGGTACGTTCCCCGATGACTATGTCTGGTTACTGGCGTGACC CGGAACGTACGGCTCAGGTTCTGTCTGGTGGTTGGCTGCGTACTGGTGAT GTTGGTACCTTCGATGAGGATGGTCACCTGCATCTGACCGATCGTCTGCA GGACATCATCATCGTTGAAGCATATAACGTCTATTCCGTGCGTGTGGAACA TGTTCTGACCGAACACCCAGATGTTCGCGCAGCTGCGGTTGTTGGCGTAC CAGATCCGGACTCTGGTGAAGCTGTTTGCGCTGCGGTTGTAGTCGCGGAT GGTGCGGATCCTGACCCTGAACACCTGCGTGCTCTGGTTCGTGATCACCT GGGTGATCTGCACGTTCCTCGCCGTGTTGAGTTCGTTCGCTCCATCCCGG TAACTCCTGCCGGCAAACCAGATAAAGTGAAAGTGCGTACCTGGTTCACC GACTAA
ml-McbA$_{procainamide}$ (CAMS)	ATGGAGAAAAAAATCTGGAGCCATCCGCAGTTCGAAAAAGGCGGATCCGG AGAAAACCTGTATTTCCAGGGCGGTTACGCTCGTCGTGTAATGGATGGTAT CGGTGAAGTAGCGGTAACTGGCGCTGGTGGTTCTGTAACTGGTGCGCGTC TGCGCCATCAGGTTCGTCTGCTGGCTCATGCTCTGACCGAAGCGGGTATT CCGCCAGGCCGTGGTGTAGCATGTCTGCATGCTAACACCTGGCGTGCGAT CGCACTGCGTCTGGCTGTTCAGGCGATTGGTTGCCACTATGTTGGTCTGC GTCCTACCGCTGCTGTTACTGAACAGGCACGCGCAATTGCGGCTGCTGAT TCTGCCGCACTGGTTTTCGAACCAAGCGTTGAAGCTCGTGCAGCTGACCT GCTGGAACGTGTTTCTGTGCCGGTTGTGCTGTCTCTGGGTCCGACCTCTC GTGGCCGTGATATCCTGGCAGCTAGCGTTCCGGAAGGTACGCCGCTGCG TTACCGTGAACACCCAGAAGGTATCGCAGTTGTAGCCTTTACTAGCGGCAC CACTGGCACCCCTAAAGGCGTTGCCCACTCCTCTACCGCTATGAGCGCTT GTGTGGATGCTGCGGTTTCCATGTACGGTCGCGGTCCTTGGCGTTTCCTG ATCCCGATCCCTCTGTCTGACCTGGGTGGCGAACTGGCACAGTGTACCCT GGCTACCGGCGGTACCGTTGTGCTGCTGGAAGAGTTCCAACCGGACGCC GTTCTGGAAGCTATCGAACGTGAACGTGCCACTCACGTGTTCCTGGCGCC GAACTGGCTGTACCAGCTGGCTGAACATCCGGCTCTGCCGCGTTCTGATC TGTCTTCTCTGCGTCGCGTTGTTTACGGCGGTGCACCGGCAGTACCATCT CGTGTAGCAGCAGCACGTGAACGTATGGGTGCTGTGCTGATGCAGAACTA CGGCACCCAGGAAGCAATGTTCATCGCAGCACTGACTCCAGACGATCACG CACGTCGTGAACTGCTGACCGCTGTAGGTCGTCCTCTGCCACACGTTGAG GTGGAAATCCGTGATGACTCTGGTGGTACTCTGCCGCGTGGTGCGGTAGG TGAAGTCTGGGTACGTTCCCCGATGACTATGTCTGGTTACTGGCGTGACC CGGAACGTACGGCTCAGGTTCTGTCTGGTGGTTGGCTGCGTACTGGTGAT GTTGGTACCTTCGATGAGGATGGTCACCTGCATCTGACCGATCGTCTGCA GGACATCATCATCGTTGAAAGCTATAACGTCTATTCCCGTCGTGTGGAACA TGTTCTGACCGAACACCCAGATGTTCGCGCAGCTGCGGTTGTTGGCGTAC CAGATCCGGACTCTGGTGAAGCTGTTTGCGCTGCGGTTGTAGTCGCGGAT

	GGTGCGGATCCTGACCCTGAACACCTGCGTGCTCTGGTTCGTGATCACCT GGGTGATCTGCACGTTCCTCGCCGTGTTGAGTTCGTTCGCTCCATCCCGG TAACTCCTGCCGGCAAACCAGATAAAGTGAAAGTGCGTACCTGGTTCACC GACTAA
ml-McbA$_{troxipide}$ (ALTV)	ATGGAGAAAAAAATCTGGAGCCATCCGCAGTTCGAAAAAGGCGGATCCGG AGAAAACCTGTATTTCCAGGGCGGTTACGCTCGTCGTGTAATGGATGGTAT CGGTGAAGTAGCGGTAACTGGCGCTGGTGGTTCTGTAACTGGTGCGCGTC TGCGCCATCAGGTTCGTCTGCTGGCTCATGCTCTGACCGAAGCGGGTATT CCGCCAGGCCGTGGTGTAGCATGTCTGCATGCTAACACCTGGCGTGCGAT CGCACTGCGTCTGGCTGTTCAGGCGATTGGTTGCCACTATGTTGGTCTGC GTCCTACCGCTGCTGTTACTGAACAGGCACGCGCAATTGCGGCTGCTGAT TCTGCCGCACTGGTTTTCGAACCAAGCGTTGAAGCTCGTGCAGCTGACCT GCTGGAACGTGTTTCTGTGCCGGTTGTGCTGTCTCTGGGTCCGACCTCTC GTGGCCGTGATATCCTGGCAGCTAGCGTTCCGGAAGGTACGCCGCTGCG TTACCGTGAACACCCAGAAGGTATCGCAGCGGTAGCCTTTACTAGCGGCA CCACTGGCACCCCTAAAGGCGTTGCCCACTCCTCTACCGCTATGAGCGCT TGTGTGGATGCTGCGGTTTCCATGTACGGTCGCGGTCCTTGGCGTTTCCT GATCCCGATCCCTCTGTCTGACCTGGGTGGCGAACTGGCACAGTGTACCC TGGCTACCGGCGGTACCGTTGTGCTGCTGGAAGAGTTCCAACCGGACGC CGTTCTGGAAGCTATCGAACGTGAACGTGCCACTCACGTGTTCCTGGCGC CGAACTGGCTGTACCAGCTGGCTGAACATCCGGCTCTGCCGCGTTCTGAT CTGTCTTCTCTGCGTCGCGTTGTTTACGGCGGTGCACCGGCAGTACCATC TCGTGTAGCAGCAGCACGTGAACGTATGGGTGCTGTGCTGATGCAGAACT ACGGCACCCAGGAAGCACTGTTCATCGCAGCACTGACTCCAGACGATCAC GCACGTCGTGAACTGCTGACCGCTGTAGGTCGTCCTCTGCCACACGTTGA GGTGGAAATCCGTGATGACTCTGGTGGTACTCTGCCGCGTGGTGCGGTAG GTGAAGTCTGGGTACGTTCCCCGATGACTATGTCTGGTTACTGGCGTGAC CCGGAACGTACGGCTCAGGTTCTGTCTGGTGGTTGGCTGCGTACTGGTGA TGTTGGTACCTTCGATGAGGATGGTCACCTGCATCTGACCGATCGTCTGCA GGACATCATCATCGTTGAAACCTATAACGTCTATTCCGTGCGTGTGGAACA TGTTCTGACCGAACACCCAGATGTTCGCGCAGCTGCGGTTGTTGGCGTAC CAGATCCGGACTCTGGTGAAGCTGTTTGCGCTGCGGTTGTAGTCGCGGAT GGTGCGGATCCTGACCCTGAACACCTGCGTGCTCTGGTTCGTGATCACCT GGGTGATCTGCACGTTCCTCGCCGTGTTGAGTTCGTTCGCTCCATCCCGG TAACTCCTGCCGGCAAACCAGATAAAGTGAAAGTGCGTACCTGGTTCACC GACTAA

Table S7. Codon table for designing site saturation mutagenesis primers. The following codons were used in the forward primers in our cell-free DNA assembly workflow to mutate a desired residue into the corresponding amino acid. While the addition of excess tRNA in CFPS reactions mitigates the negative effects of unoptimized codons, we used the most prevalent codon found in *E. coli* for the compatibility of *in vivo* expression and to prevent the need for re-optimizing the entire sequence.

Amino Acid	Codon
A	GCG
R	CGT
N	AAC
D	GAT
C	TGC
Q	CAG
E	GAA
G	GGC
H	CAT
I	ATT
L	CTG
K	AAA
M	ATG
F	TTT
P	CCG
S	AGC
T	ACC
W	TGG
Y	TAT
V	GTG

Table S8. Thermocycler parameters for cell-free DNA assembly. The following thermocycler parameters were consistent throughout this study, with extension time being the only variable changing to compensate for different amplicon lengths. The first step uses touchdown PCR, in which the initial annealing temperature decreases by 1 °C each cycle until a final set temperature is reached.

PCR 1 parameters:

Step	Temp (°C)	Time (min:sec)
Initial Denaturation	98	3:00
6x	98	0:30
	70 (-1 °C/cycle)	0:30
	72	20s/kbp
20x	98	0:30
	64	0:30
	72	20s/kbp
Final Extension	72	10:00
Hold	12	∞

PCR 2 parameters:

Step	Temp (°C)	Time (min:sec)
Initial Denaturation	98	3:00
30x	98	0:30
	68	0:30
	72	20s/kbp
Final Extension	72	10:00
Hold	12	∞

Table S9. Primers for site saturation mutagenesis of wt-McbA. The base forward (fwd) and reverse (rvs) primers for site saturation mutagenesis of wt-McbA using our cell-free DNA assembly workflow. While there is only a single reverse primer for saturating a single residue, the forward primer carries the desired mutation (so there are subsequently 20 forward primers per residue). We label this flexible position as 'NNN', indicating that all 20 codons found in **Table S7** are inserted here.

Residue	Direction	Sequence
Y97	fwd	CGATTGGTTGCCACNNNGTTGGTCTGCG
	rvs	GTGGCAACCAATCGCCTGAACA
R101	fwd	CCACTATGTTGGTCTGNNNCCTACCGC
	rvs	CAGACCAACATAGTGGCAACCAATCG
P102	fwd	TGTTGGTCTGCGTNNNACCGCTG
	rvs	ACGCAGACCAACATAGTGGCAAC
T103	fwd	GGTCTGCGTCCTNNNGCTGCTG
	rvs	AGGACGCAGACCAACATAGTGGC
V177	fwd	CAGAAGGTATCGCANNNGTAGCCTTTACTAGCG
	rvs	TGCGATACCTTCTGGGTGTTCACG
V178	fwd	GAAGGTATCGCAGTTNNNGCCTTTACTAGCGG
	rvs	AACTGCGATACCTTCTGGGTGTTCA
A179	fwd	GGTATCGCAGTTGTANNNTTTACTAGCGGC
	rvs	TACAACTGCGATACCTTCTGGGTGTTC
T181	fwd	GCAGTTGTAGCCTTTNNNAGCGGCACCA
	rvs	AAAGGCTACAACTGCGATACCTTCTGG
V191	fwd	CACCCCTAAAGNNNCGGCCCACTC
	rvs	GCCTTTAGGGGTGCCAGTGGT
H193	fwd	TAAAGGCGTTGCCNNNTCCTCTACCG
	rvs	GGCAACGCCTTTAGGGGTGC
A197	fwd	CCCACTCCTCTACCNNNATGAGCGC
	rvs	GGTAGAGGAGTGGGCAACGC
M198	fwd	CTCCTCTACCGCTNNNAGCGCTTGTGTG
	rvs	AGCGGTAGAGGAGTGGGCAAC
C201	fwd	GCTATGAGCGCTNNNGTGGATGCTGC
	rvs	AGCGCTCATAGCGGTAGAGGAG
A205	fwd	CTTGTGTGGATGCTNNNGTTTCCATGT
	rvs	AGCATCCACACAAGCGCTCATAG
Y209	fwd	TGCGGTTTCCATGNNNGGTCGCG
	rvs	CATGGAAACCGCAGCATCCACA
I220	fwd	GTTTCCTGATCCCGNNNCCTCTGTCTGAC
	rvs	CGGGATCAGGAAACGCCAAGG
P221	fwd	TCCTGATCCCGATCNNNCTGTCTGACC
	rvs	GATCGGGATCAGGAAACGCCAAG
D224	fwd	CGATCCCTCTGTCTNNNCTGGGTGG
	rvs	AGACAGAGGGATCGGGATCAGGA
L225	fwd	TCCCTCTGTCTGACNNNGGTGGC
	rvs	GTCAGACAGAGGGATCGGGATCAG
E228	fwd	GACCTGGGTGNNNCGCTGGCAC
	rvs	GCCACCCAGGTCAGACAGAGG
L229	fwd	CTGGGTGGCGAANNNGCACAGTG

	rvs	TTCGCCACCCAGGTCAGACAG
C232	fwd	CGAACTGGCACAGNNNACCCTGGC
	rvs	CTGTGCCAGTTCGCCACCC
E244	fwd	CGTTGTGCTGCTGNNNGAGTTCCAACC
	rvs	CAGCAGCACAACGGTACCGC
E245	fwd	TGTGCTGCTGGAANNNTTCCAACCG
	rvs	TTCCAGCAGCACAACGGTACC
F246	fwd	GCTGCTGGAAGAGNNNCAACCGGAC
	rvs	CTCTTCCAGCAGCACAACGGTAC
F264	fwd	GCCACTCACGTGNNNCTGGCG
	rvs	CACGTGAGTGGCACGTTCACG
L265	fwd	CCACTCACGTGTTCNNNGCGC
	rvs	GAACACGTGAGTGGCACGTTCA
A266	fwd	CTCACGTGTTCCTGNNNCCGAA
	rvs	CAGGAACACGTGAGTGGCACG
W269	fwd	TGGCGCCGAACNNNCTGTACC
	rvs	GTTCGGCGCCAGGAACACG
V292	fwd	CGTCGCGTTGTTNNNGGCGGTG
	rvs	AACAACGCGACGCAGAGAAGAC
G293	fwd	GTCGCGTTGTTTACNNNGGTGC
	rvs	GTAAACAACGCGACGCAGAGAAGA
G294	fwd	CGTTGTTTACGNNNCGGCACCG
	rvs	GCCGTAAACAACGCGACGC
A295	fwd	TGTTTACGNNNGTGCACCGG
	rvs	ACCGCCGTAAACAACGCGAC
P296	fwd	CGGCGGTGCANNNGCAG
	rvs	TGCACCGCCGTAAACAACGC
A297	fwd	CGGTGCACCGNNNGTACCATCTC
	rvs	CGGTGCACCGCCGTAAACA
Q315	fwd	TGCTGTGCTGATGNNNAACTACGGC
	rvs	CATCAGCACAGCACCCATACGTTC
N316	fwd	TGTGCTGATGCAGNNNTACGGCACC
	rvs	CTGCATCAGCACAGCACCCATAC
Y317	fwd	TGCTGATGCAGAACNNNGGCACCC
	rvs	GTTCTGCATCAGCACAGCACCC
G318	fwd	CTGATGCAGAACTACNNNACCCAGGAA
	rvs	GTAGTTCTGCATCAGCACAGCACC
T319	fwd	GCAGAACTACGNNNCGCAGGAAGC
	rvs	GCCGTAGTTCTGCATCAGCACAG
Q320	fwd	GAACTACGGCACCNNNGAAGCAGC
	rvs	GGTGCCGTAGTTCTGCATCAGC
E321	fwd	TACGGCACCCAGNNNGCAGCTTTCA
	rvs	CTGGGTGCCGTAGTTCTGCATC
A323	fwd	CACCCAGGAAGCANNNTTCATCGCAG
	rvs	TGCTTCCTGGGTGCCGTAGT
F324	fwd	CCAGGAAGCAGCTNNNATCGCAGCA
	rvs	AGCTGCTTCCTGGGTGCC
A341	fwd	GTGAACTGCTGACCNNNGTAGGTCGT
	rvs	GGTCAGCAGTTCACGACGTGC

M375	fwd	GTACGTTCCCCGNNNACTATGTCTGGTTACTGG
	rvs	CGGGGAACGTACCCAGACTTCA
T376	fwd	ACGTTCCCCGATGNNNATGTCTGGTTACTGG
	rvs	CATCGGGGAACGTACCCAGACT
D400	fwd	GCTGCGTACTGGTNNNGTTGGTACCTTC
	rvs	ACCAGTACGCAGCCAACCAC
L412	fwd	TGGTCACCTGCATNNNACCGATCGTC
	rvs	ATGCAGGTGACCATCCTCATCGAAG
D414	fwd	CCTGCATCTGACCNNNCGTCTGCAG
	rvs	GGTCAGATGCAGGTGACCATCCT
R415	fwd	TGCATCTGACCGATNNNCTGCAGGAC
	rvs	ATCGGTCAGATGCAGGTGACCATC
I421	fwd	TGCAGGACATCATCNNNGTTGAAGCATATAACGTC
	rvs	GATGATGTCCTGCAGACGATCGGT
E423	fwd	GGACATCATCATCGTTNNNGCATATAACGTCTATTCCCG
	rvs	AACGATGATGATGTCCTGCAGACGA
A424	fwd	CATCATCATCGTTGAANNNTATAACGTCTATTCCCGTCG
	rvs	TTCAACGATGATGATGTCCTGCAGAC
Y425	fwd	ATCATCGTTGAAGCANNNAACGTCTATTCCCGTCGTG
	rvs	TGCTTCAACGATGATGATGTCCTGC
N426	fwd	CATCGTTGAAGCATATNNNGTCTATTCCCGTCGTG
	rvs	ATATGCTTCAACGATGATGATGTCCTGC
R430	fwd	GCATATAACGTCTATTCCNNNCGTGTGGAACATG
	rvs	GGAATAGACGTTATATGCTTCAACGATGATGATG
L487	fwd	ATCACCTGGGTGATNNNCACGTTCCTC
	rvs	ATCACCCAGGTGATCACGAACCAG
P503	fwd	CCATCCCGGTAACTNNNGCCGG
	rvs	AGTTACCGGGATGGAGCGAACG
A504	fwd	CCCGGTAACTCCTNNNGGCAAAC
	rvs	AGGAGTTACCGGGATGGAGCG
G505	fwd	GGTAACTCCTGCCNNNAAACCAGATAAAGT
	rvs	GGCAGGAGTTACCGGGATGGAG
K506	fwd	CTCCTGCCGNNNCGCCAGATAAAGTGAAAGT
	rvs	GCCGGCAGGAGTTACCGG
P507	fwd	CCTGCCGGCAAANNNGATAAAGTGAAAGTG
	rvs	TTTGCCGGCAGGAGTTACCG
D508	fwd	GCCGGCAAACCANNNAAAGTGAAAGTGCG
	rvs	TGGTTTGCCGGCAGGAGTTAC

Table S10. Primers for site saturation mutagenesis of muGFP. The forward (fwd) and reverse (rvs) primers for site saturation mutagenesis of muGFP using our cell-free DNA assembly workflow. We also include the primers used in the optimization of the homologous overlap between the two primers found in **Fig. S3**. The temperature next to the primer for Y66 corresponds to the melting temperature of the overlap.

Residue	Direction	Sequence
Y66		CCACTCTTACATATGGTGTGTTGTGCTTTAGC
	fwd – 27 °C	TACCACTCTTACATATGGTGTGTTGTGCTTTA
	fwd – 33 °C	TGTTACCACTCTTACATATGGTGTGTTGTGCT
	fwd – 42 °C	CTCTTGTTACCACTCTTACATATGGTGTGTTGTG
	fwd – 48 °C	CCTACTCTTGTTACCACTCTTACATATGGTGTGTT
	fwd – 53 °C	G
	rvs	TGTAAGAGTGGTAACAAGAGTAGGCC
L69	fwd	CTCTTACATATGGTGTGTTGTGCTTTAGCCG
	rvs	CACACCATATGTAAGAGTGGTAACAAGAG
Y164	fwd	AATGGGATCAAAGCATACTTCAAAATCCGC
	rvs	TGCTTTGATCCCATTTTTTTGCTTATCAG
T203	fwd	CAATCACTACCTTAGCACACAGTCGGTATT
	rvs	GCTAAGGTAGTGATTGTCTGGCAAC

Table S11. Primers for amplifying LETs using pJL1 plasmid as a backbone. These primers are universally used to amplify LETs off pJL1 containing any gene of interest. They add approximately 300 base pairs both upstream and downstream of the coding region to help protect against exonucleases present in the *E. coli* lysate.

Direction	Sequence
LET_fwd	CTGAGATACCTACAGCGTGAGC
LET_rvs	CGTCACTCATGGTGATTTCTCACTTG

Table S12. BLOSUM50 reduced amino libraries. We randomly selected four sets of 10 amino acids from groupings derived from the BLOSUM50 matrix. These groupings were used in the retrospective analysis found in **Fig. 4**. To trim the datasets, only single mutations containing one of the following amino acids were included in that training set. Depending on the amino acid at each residue for wt-McbA, this sometimes led to slight changes (+/- 4 data points max) in the total number of samples in the set.

Group 1	Group 2	Group 3	Group 4
L	I	M	V
C	C	C	C
A	A	A	A
G	G	G	G
S	S	T	T
P	P	P	P
F	Y	F	W
E	D	N	Q
K	R	R	K
H	H	H	H

Table S13. CAS numbers of select compounds used in this study.

Product	Acid	Amine	Amide
Moclobemide	74-11-3	2038-03-1	71320-77-9
Metoclopramide	7206-70-4	100-36-7	364-62-5
Cinchocaine	10222-61-4	100-36-7	85-79-0
Itopride	93-07-2	20059-73-8	122892-31-3
Declopramide	2486-71-7	100-36-7	891-60-0
Trimethobenzamide	118-41-2	20059-73-8	554-92-7
(S)-Sulpiride	22117-85-7	22795-99-9	15676-16-1
Procainamide	150-13-0	100-36-7	51-06-9
Troxipide	118-41-2	334618-23-4	30751-05-4

Uncropped Protein Gel Images

For Supplementary Figure 6:

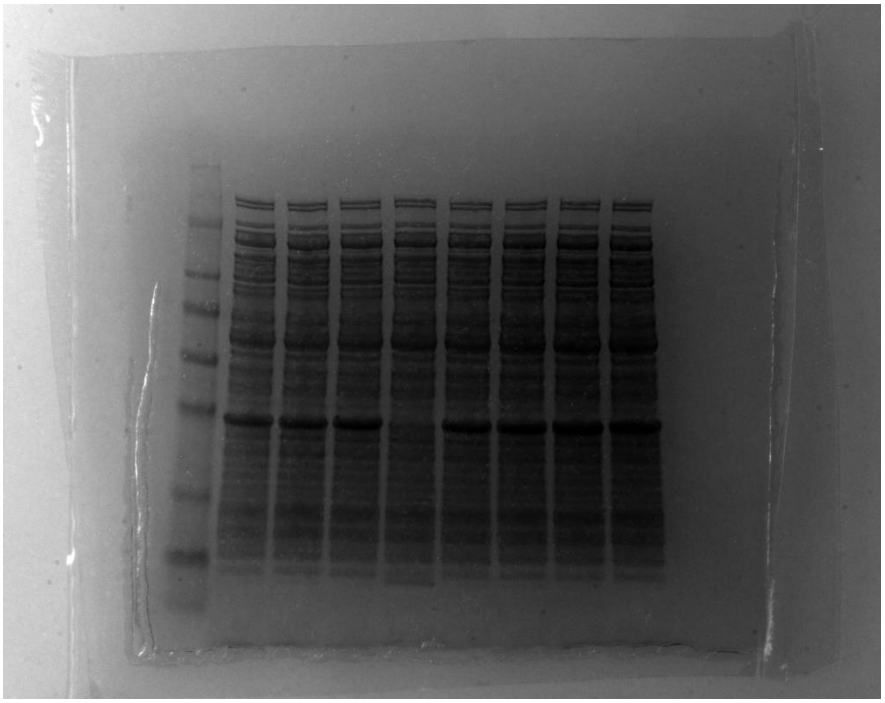

For Supplementary Figure 8:

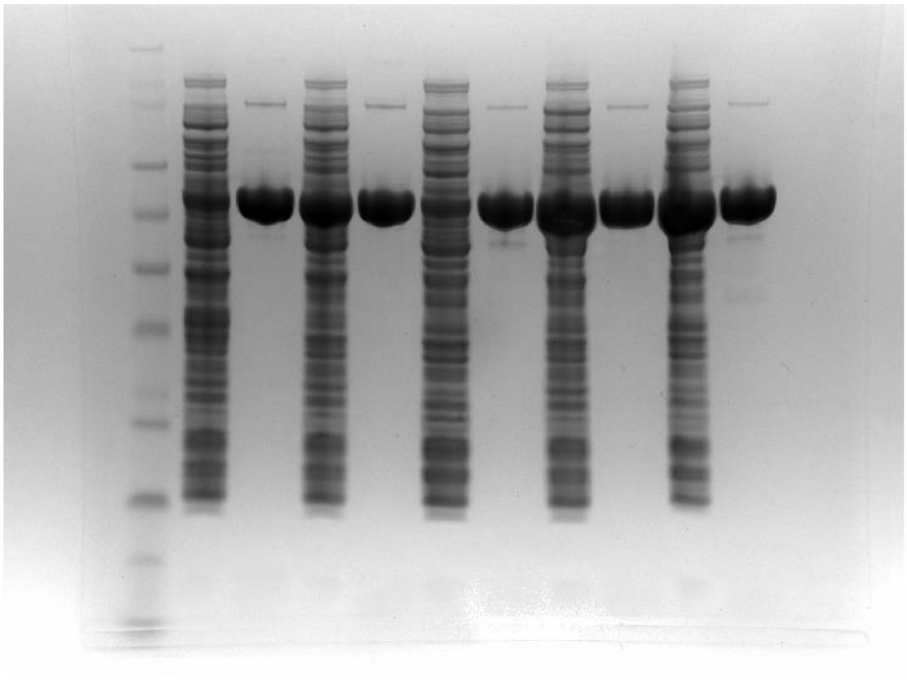

Uncropped DNA Gel Images

For Supplementary Figure 3:

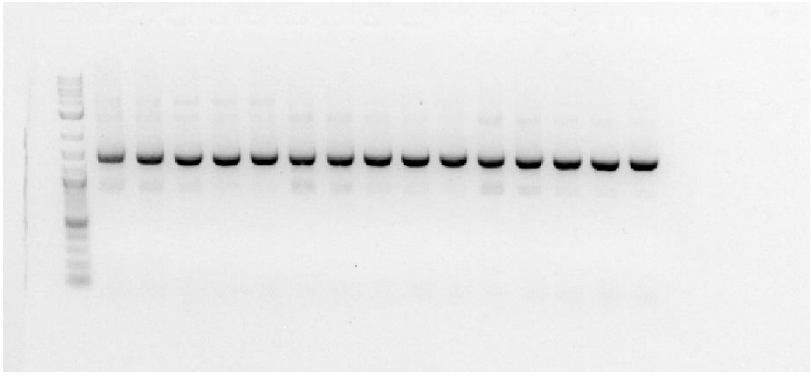

For Supplementary Figure 4:

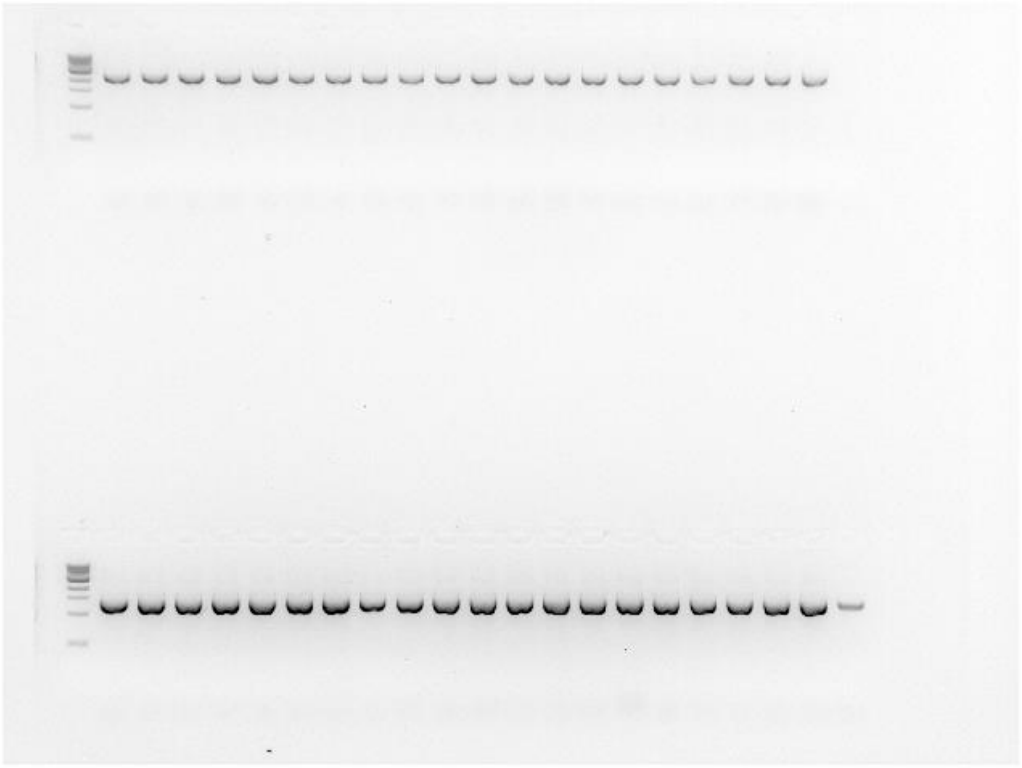

Supplementary References

1. Petchey, M. R., Rowlinson, B., Lloyd, R. C., Fairlamb, I. J. S. & Grogan, G. Biocatalytic Synthesis of Moclobemide Using the Amide Bond Synthetase McbA Coupled with an ATP Recycling System. *Acs Catal* **10**, 4659–4663 (2020).

2. Mordhorst, S., Maurer, A., Popadić, D., Brech, J. & Andexer, J. N. A Flexible Polyphosphate-Driven Regeneration System for Coenzyme A Dependent Catalysis. *Chemcatchem* **9**, 4164–4168 (2017).